AGU ADVANCING EARTH AND SPACE SCIENCE

Earth and Space Science

RESEARCH ARTICLE
10.1029/2022EA002359

Attribution of Observed Periodicity in Extreme Weather Events in Eastern North America

C. R. Walsh[1] and **R. T. Patterson**[1]

[1]Department of Earth Sciences, Carleton University, Ottawa, ON, Canada

Key Points:

- Extreme weather events across eastern North America from 1881 to 2020 were analyzed for trends and patterns
- Eastern North America exhibits three distinct extreme weather subregions
- Cyclic patterns in extreme weather were attributed to various large-scale climate oscillations

Supporting Information:

Supporting Information may be found in the online version of this article.

Correspondence to:

C. R. Walsh,
carling.walsh@carleton.ca

Citation:

Walsh, C. R., & Patterson, R. T. (2022). Attribution of observed periodicity in extreme weather events in eastern North America. *Earth and Space Science*, *9*, e2022EA002359. https://doi.org/10.1029/2022EA002359

Received 1 APR 2022
Accepted 6 JUN 2022

Author Contributions:

Conceptualization: C. R. Walsh, R. T. Patterson
Formal analysis: C. R. Walsh
Funding acquisition: R. T. Patterson
Investigation: C. R. Walsh
Methodology: C. R. Walsh, R. T. Patterson
Supervision: R. T. Patterson
Writing – original draft: C. R. Walsh
Writing – review & editing: C. R. Walsh, R. T. Patterson

Abstract Instrumental weather records (1880–2020s) from eastern North America were analyzed to characterize the regional patterns and drivers of seasonal extreme weather (snow, rain, high and low temperatures). Using agglomerative hierarchical clustering of extreme weather data, the region was divided into three subregions that are influenced by coastal-marine gradients and latitudinal factors. Subsequent analyses were performed on high-quality stations from each subregion and results compared between one another. Long-term locally weighted linear regressions delineated long-term changes in extreme weather, and a combination of spectral analysis, continuous wavelet transforms, and cross wavelet transforms were used to identify periodic components in the data. Regional extreme weather is generally periodic, composed of interannual to interdecadal-scale oscillations and driven by several natural climatic oscillations. The most important such oscillation is the 11-year Schwabe Solar Cycle, which has a strong and continuous effect on regional extreme weather. The Pacific Decadal Oscillation and Quasi Biennial Oscillation also show considerable influence, but intermittently. The El Niño Southern Oscillation, the Arctic Oscillation, and the North Atlantic Oscillation all have a weaker but interrelated influence. While the Atlantic Multidecadal Oscillation showed the weakest overall influence on regional extreme weather, it demonstrated a clear spatial gradient across the region, unlike the aforementioned oscillations. Long-term changes in regional extreme weather are not generally important, in that a sustained increase or decrease in extreme weather events is not usually characteristic of the weather records. The primary exception to this result is for extreme minimum temperature events, whose frequency has slightly decreased since the 1880s.

1. Introduction

Extreme weather events can be detrimental both environmentally and economically; the occurrence of extreme events such as snow storms and heatwaves can negatively impact public health and safety, ecological health, and infrastructure, and have been ranked among the top global risk factors, both by economic and environmental standards (Dolney & Sheridan, 2006; Smith & Sheridan, 2019; Stockwell et al., 2020; Van de Pol et al., 2017; World Economic Forum, 2019; Znachor et al., 2008). Despite recent popular attention to such weather events, there is a dearth of relevant studies conducted at a regional level, as opposed to more localized scales (e.g., cities and environs) or global scales. For eastern North America, analyses of extreme weather events are somewhat limited, and a large portion of the body of research pertains to the relation of extreme weather to public health and ecological factors (Bailey & Secor, 2016; McMichael, 2015; Paterson et al., 2012; Reid et al., 2007). Some studies do assess the changes in various extreme weather parameters over time. For example, several authors have examined the changes in extreme temperatures or precipitation through the 20th and early 21st centuries, revealing that both extreme temperature and precipitation values have increased (Ahmed et al., 2014; Allen et al., 2015; B. Bonsal et al., 2001; B. R. Bonsal et al., 2001; Shephard et al., 2014; Soulis et al., 2016; Yagouti et al., 2008; Zhang et al., 2001). The frequency and long term changes in when and how often these extreme temperature and precipitation events occur, as well as their potential drivers, are less frequently explored.

The potential drivers of regional climate that may be detected in instrumental weather records are limited to the interannual to multidecadal scales, as instrumental records in eastern North America typically do not extend earlier than the late 19th century. This time frame excludes the ability to robustly analyze the effects of many climate phenomena at the century-scale or greater. Due to the global nature of teleconnections there are many oscillations that may have influence on the regional climate. However, a large body of research (Bonsal & Shabbar, 2011; Chandran et al., 2016; Kwon et al., 2006; Ogurtsov et al., 2008; Thiombiano et al., 2017; Yang et al., 2019; Zhang et al., 2010) suggests that there are seven key oscillations that most significantly impact eastern North American climate. These are: the Schwabe Solar Cycle (SSC), the Atlantic Multidecadal Oscillation

(AMO), the Pacific Decadal Oscillation (PDO), the El Niño Southern Oscillation (ENSO), the Arctic Oscillation (AO), the North Atlantic Oscillation (NAO), and the Quasi–Biennial Oscillation (QBO). The characteristics of these seven oscillations are summarized in Table 1.

The principal objective of this paper was to characterize the drivers of extreme weather (snow, rain, high and low temperatures) in eastern North America with regards to any cyclicities or long-term trends present, with particular emphasis on the seven oscillations described above. A secondary goal was to determine whether there was any regional variation in the expression of extreme weather in eastern North America. To achieve these goals agglomerative hierarchical clustering was used on the extreme weather data to detect any regional variability. In addition, several time series analysis techniques were employed on extreme weather data derived from select instrumental stations from across the region. Long-term locally weighted linear regressions (LOWESS), red noise-spectral analysis, continuous wavelet transforms (CWTs) and cross wavelet transforms (XWTs) were applied to the instrumental weather records. XWTs were calculated between the instrumental weather records and the each of the seven climatic oscillation time series.

2. Methods

2.1. Defining Extreme Weather

Previous researchers have used a variety of definitions of extreme weather events. In this study, weather events are classified as extreme if they fall outside of two standard deviations from the mean of all weather events ($\mu \pm 2\sigma$, where μ is the mean and σ is the standard deviation) at a given location (Frei et al., 2015; Marquardt Collow et al., 2016; Wang et al., 2015; Yagouti et al., 2008). This definition is commonly referred to as the 95th percentile definition, based on events following a normal distribution. Univariate data is used, with the four weather variables of interest here considered separately: extreme events for maximum temperature, minimum temperature, rainfall, and snowfall. As the chosen approach provides discrete counts of events based on the statistical distribution as considered for one location, it is ideal when multiple locations are compared. It is also ideal to assess single-day extremes, though multi-day extreme events can also be detected using this method when corrections are applied to ensure that all events are mutually exclusive (Frei et al., 2015).

2.2. Data Acquisition and Preprocessing

Weather station data was obtained from Environment and Climate Change Canada (2020) and the National Oceanic and Atmospheric Association (2020) for 90 locations across eastern North America, with each record containing daily resolution maximum and minimum temperature, rainfall, and snowfall data.

To assess how patterns in extreme weather occurrences might differ across the greater region, data from the 90 stations (listed in Table S1 in Supporting Information S1) was analyzed using agglomerative hierarchical clustering with the Ward linkage (Ward, 1963; Figures 1 and 2). The categories used in the clustering algorithm included observations of each of the seasonal extreme weather variables at each location from 1936 to 1999 (the period in which all 90 stations had data), as well as station coordinates. Non-metric multidimensional scaling (NMDS, Kruskal, 1964) was carried out to further investigate and verify the cluster results by reducing the clustered data set to two dimensions by minimizing the dissimilarity in the input dimensions, such that it can be readily represented on a scatter plot (Figure 3).

Based on the cluster analysis and NMDS three distinct subregions were recognized. Within each distinct subregion, 4–7 stations were selected. The basis of this selection is three-fold; first, a station's record must be long-running with minimal missing data. Second, the assemblage must be geographically representative of the subregion, that is, not unduly clustered in space and representing a variety of possible localized climates (e.g., not all coastal stations). Lastly, the number of stations selected from each subregion varied based on the subregion's size; thus, the most geographically constrained region was represented by only four sample stations, whereas the broadest subregion was represented by seven sample stations. Two of the subregions are grouped along the Atlantic coast and the third represents the continental portion of eastern North America. These regions are termed here as the Maritime Region (MR), Southern Region (SR), and Continental Region (CR). These subregions and their constituent sample stations are given in Figure 1.

Table 1
Descriptions and Regional Effects of Various Climatic Oscillations Known to Impact the Region of Eastern North America

Climatic oscillation	Notation	Cycle length (years)	Description	Common impact on eastern North American climate	Citations
Schwabe Solar Cycle	SSC	~11, 8–17	An oscillation in the annual number of sunspots occurring, relating to total solar irradiance. The increases in total solar irradiance and UV irradiance during sunspot maxima drive dynamic changes in global stratospheric and tropospheric temperatures.	Increases in temperature during sunspot maxima, decreases in temperature during sunspot minima. Various links to precipitation and precipitation-related parameters.	Lassen and Friis-Christensen (1995); Rind et al. (2008); Lockwood (2012); Hathaway (2015)
Atlantic MultidecadalOscillation	AMO	~64, 50–90, 16–24 subharmonics	An oscillation in the circulation pattern of warm and cool Atlantic ocean surface waters. Warm (AMO+) phases occurred from ~1925–1965 and ~1990-present, cool (AMO-) phases occurred from ~1900–1925 and ~1965–1990.	AMO+ is associated with increased temperatures, decreased precipitation, and greater drought probability.	Schlesinger and Ramankutty (1994); Enfield et al. (2001); Knight et al. (2006); Dima and Lohmann (2007); Feng et al. (2011); Knudsen et al. (2011); Ruiz-Barradas et al. (2013); Alexander et al. (2014)
Pacific Decadal Oscillation	PDO	~interannual–multidecadal; strongest oscillations in the 15–25 years and 50–70 years bands	Characterized by fluctuations in sea-surface temperature; during PDO + phases, the western mid-latitude Pacific cools, whereas eastern mid- and low-latitude Pacific warms. Interannual fluctuations in the PDO are linked to ENSO and Aleutian Low variability.	PDO + phases are associated with decreased precipitation in the Great Lakes region and cooler temperatures in southeastern North America. Opposite patterns occur during PDO-.	Trenberth (1990); Latif and Barnett (1994); Minobe (1997, 1999); Mantua and Hare (2002)
North Atlantic Oscillation	NAO	poorly defined, typically interannual–interdecadal	A localized oscillation in the sea level pressure differential between the Azores High and the Icelandic Low in the northern Atlantic Ocean.	NAO + phases are typically associated with more moderate temperatures and wetter conditions in eastern North America, and drier, more extreme temperatures during NAO- phases.	Hurrell (1995); Hurrell et al. (2001, 2003); Olsen et al. (2012)

Table 1
Continued

Climatic oscillation	Notation	Cycle length (years)	Description	Common impact on eastern North American climate	Citations
Arctic Oscillation	AO	poorly defined, typically interannual–interdecadal	A broad oscillation in sea-level pressure in the Northern Hemisphere, occurring in an annular band around the northern mid-latitudes. During its positive phase, the AO supports a low-amplitude jet stream, during an AO- phase the jet-stream becomes a high-amplitude waveform. The localized NAO is a constituent of the broad scale AO.	Brings cool Arctic air to the mid-latitudes during AO+; cool Arctic airmasses travel further south into North America during AO-.	Deser (2000); Ambaum et al. (2001); Rogers and McHugh (2002); Li et al. (2017)
El Nino Southern Oscillation	ENSO	2–10	An oscillation characterized by the changes in sea surface temperatures in the tropical Pacific. Driven by the variation in strength of tropical trade winds—causing greater or weaker degrees in the upwelling of cool, deep ocean water during El Nino (ENSO+) and La Nina (ENSO-), respectively—this oscillation influences many regions of the world via various teleconnections.	Warmer, drier conditions during El Nino; cooler, wetter conditions during La Nina.	Philander (1983); Ropelewski and Halpert (1986); Philander (1989); Moy et al. (2002); Hu and Feng (2012)
Quasi-Biennial Oscillation	QBO	2.1–2.4	The oscillation between westerly and easterly winds in the equatorial stratosphere. Air masses then propagate downward to the troposphere and are subsequently propagated poleward via teleconnections with surface waves.	Cooler temperatures during the westerly (QBO+) phase, warmer temperatures during the easterly (QBO-) phase.	Lindzen and Holton (1968); Dunkerton (1997); Baldwin et al. (2001); Chattopadhyay and Bhatla (2002); Sharma and Magnuson (2014); Patterson and Swindles (2015); Gray et al. (2018)

For each of the exemplary stations in the three subregions, the weather records were subdivided into meteorological seasons (winter (DJF), spring (MAM), summer (JJA), and autumn (SON)). The seasonal weather records were then processed to extract discrete counts of each extreme maximum temperature, minimum temperature, rainfall, and snowfall events per season per year, based on the 95th percentile definition of extreme weather as outline in Section 2.1. For both rainfall and snowfall, only non-zero precipitation days were included in the calculation to avoid skewing the event distributions. The seasonal extreme weather records were then subjected to various time series analysis techniques to assess the presence of trends and patterns in extreme weather across eastern North America.

Time series representing seven climatic drivers known to affect regional climate (SSC, AMO, PDO, NAO, AO, ENSO, and QBO) were obtained from NCAR (2013), Deser et al. (2016), Hurrell and NCAR (2020), NCAR (2020), Trenberth and NCAR. (2020), SILSO (2021), and Trenberth et al. (2021). These climatic drivers were used in conjunction with the weather station data during time series analysis to assess the presence of cyclical relationships.

2.3. Time Series Analysis

To assess long-term non-cyclical trends in extreme weather, LOWESS were carried out on each seasonal extreme weather records. LOWESS smoothing over 20 year periods provides a general sense of the long-term trends and

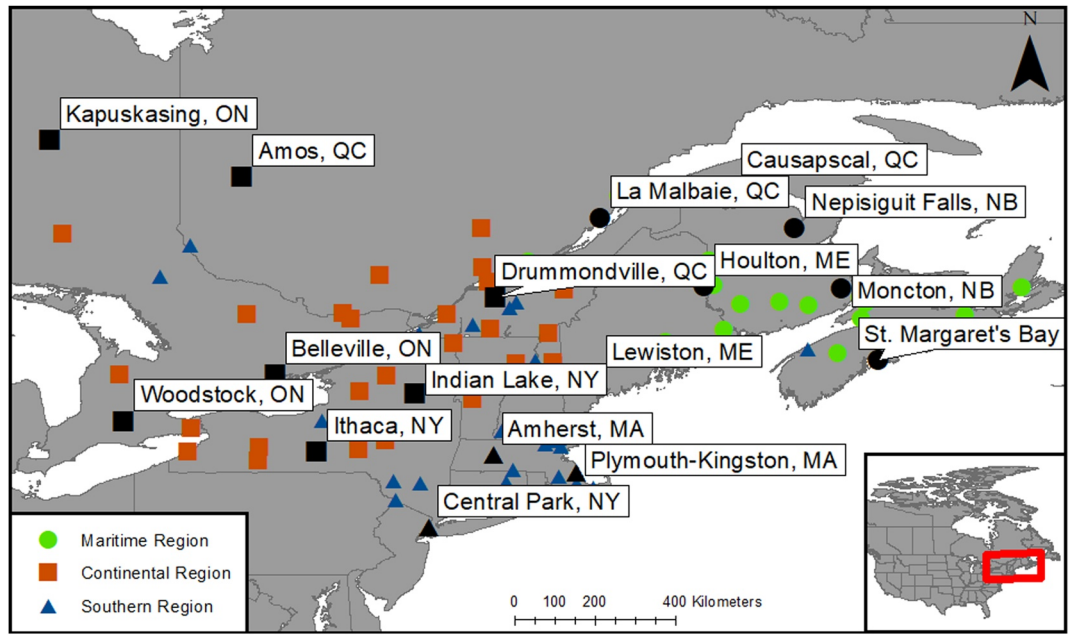

Figure 1. Map of eastern North America. All 90 weather stations used in clustering analysis are displayed, with symbols depicting the three subregions they belong to. The sample stations from each subregion used in time series analysis are labeled.

fluctuations in the occurrence of extreme weather events (Cleveland, 1979, 1981). Bootstrapping (1,000 replicates) was used to compute the 95% confidence interval on the LOWESS models.

The assessment of cyclical patterns in extreme weather is summarized as follows:

1. Red noise spectral analysis yields periodograms which identify the periodicities that account most for a time series' spectral power (shown as peaks on the periodogram).
2. A CWT expands on the periodogram, by identifying time-varying ranges of elevated spectral power, thus allowing to interpret *when* in the time series a given periodicity has greater spectral power, and thus greater importance.
3. A cross wavelet transform (XWT) expands on a CWT by finding time-varying ranges where two signals—in this case, a weather record and a climatic driver—share trends in spectral power.

Red noise spectral analysis is based on Thomson's multitaper method (Thomson, 1982), which compares a series of waveforms to an input signal, realizing the various oscillatory patterns within the input signal. Using a bootstrapping approach, these oscillatory patterns are then compared against the red noise spectrum of the input signal (denoted as AR1) and various confidence intervals (Dorothée, 2020; Schulz & Mudelsee, 2002). While this form of analysis gives easily interpretable peaks on the resultant periodogram, it assumes stationarity (i.e., no change in constituent oscillations over the length of the time series), which is rarely the case.

CWTs are used to build on spectral analysis as they yield a three-dimensional solution which is represented as "map" of spectral power on a time-frequency coordinate system. This approach compares a wavelet of varying frequencies (here, the Morlet wavelet is used) to the input signal over time (Grinsted et al., 2004; Schulz & Mudelsee, 2002; Torrence & Compo, 1998). A CWT plot helps to identify which periodicities are more prominent at a given time in the record.

The two previous steps can be used equally on a time series representing a climatic driver; however, comparing two periodograms or CWT plots by inspection to identify similarities between a weather record and a climatic record is not statistically rigorous, particularly as climatic drivers sometimes lack a discrete period and instead have a series of various frequency bands. Instead, the XWT is used to compare one time series to another. While similar to the CWT in that it compares varying frequencies of a wavelet to input signals through time, the purpose of an XWT is to calculate which oscillations are common between the two input signals (Grinsted et al., 2004).

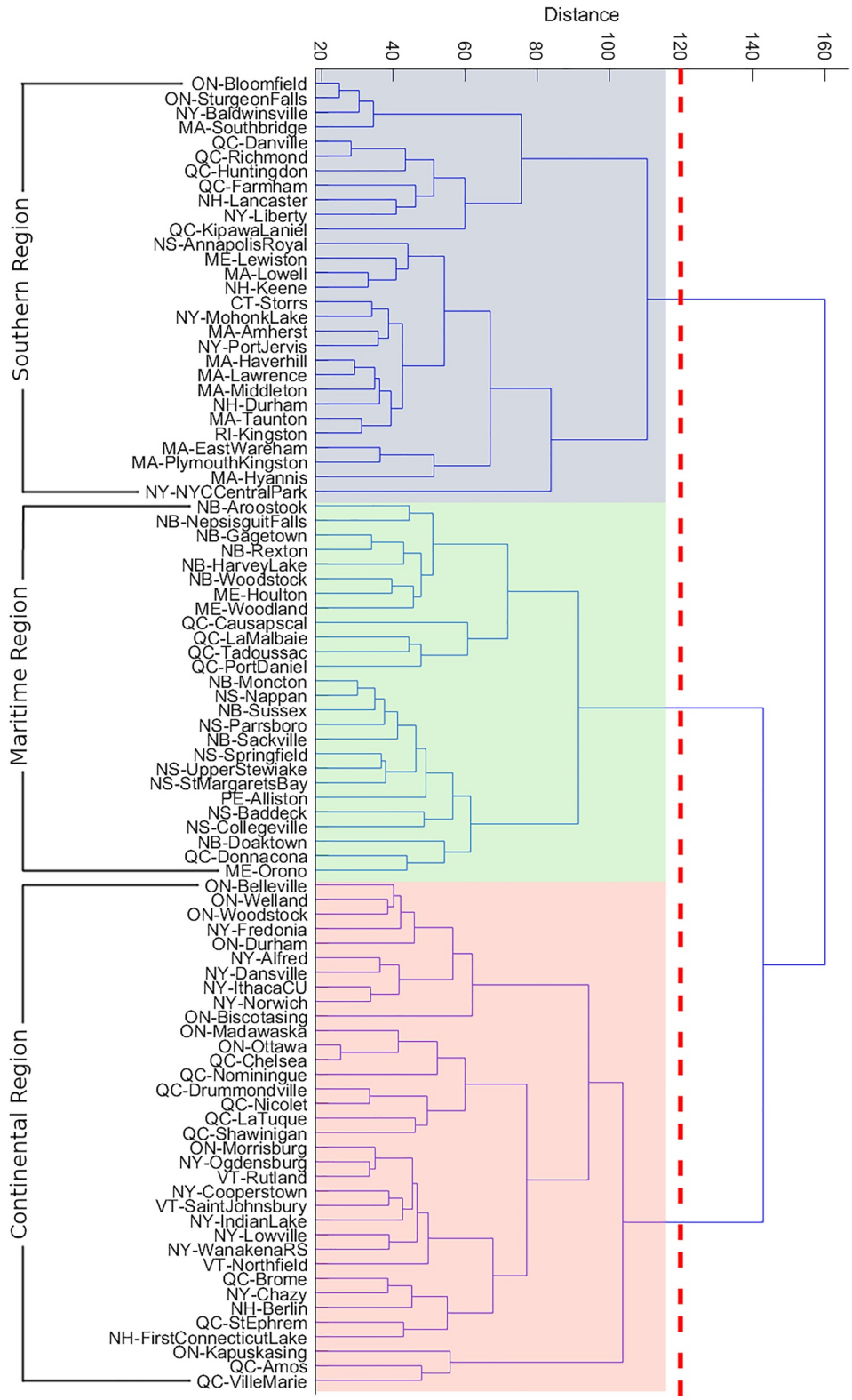

Figure 2. Ward linkage cluster analysis showing three clusters, nodes labeled with weather station names. Colors correspond to those shown in map view in Figure 1.

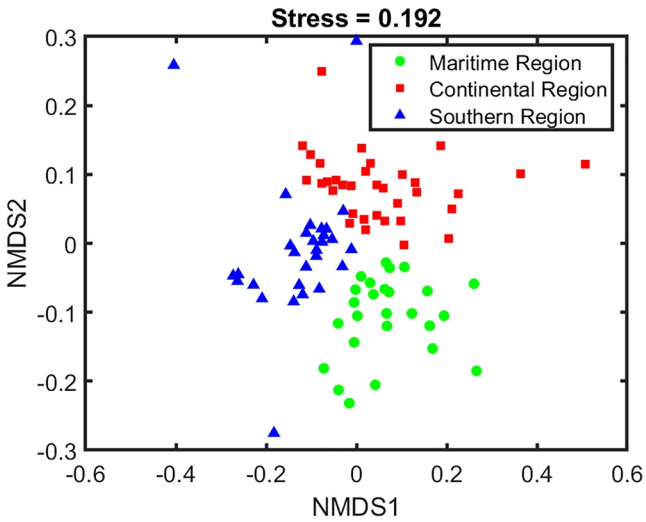

Figure 3. Non-metric multidimensional scaling of extreme weather records in eastern North America. Colors correspond to those shown in map view in Figure 1.

An XWT's output is similar to that of a CWT, but the magnitude of a region in the time-frequency coordinate system corresponds to how much the two inputs are correlated at a given time for a given frequency.

Using an integrated approach between spectral analysis, CWTs, and XWTs permits for a more rigorous assessment of what climatic drivers are at play. For example, one may identify certain significant peaks on periodograms, then identify on a CWT when in the time series these peaks have greater power, and then identify with an XWT whether the frequency content of the time series is similar that of a climatic driver. Conversely, one may work backwards, that is, to confirm that a given correlation to a climatic driver is something that is identifiable from original weather record by itself with the aid of a periodogram or CWT plot. Note that it is difficult to authoritatively assign cause for a certain spectral peak on a periodogram to a given climatic driver without these steps, as multiple drivers have similar frequency bands.

3. Results

A full array of figures depicting the LOWESS regressions, spectral analysis, CWTs and XWTs are available as Figures in Supporting Information S1. The results and discussion feature those figures which are either generally representative of a trend in question, modified subsets of the supplementary figures to better showcase a trend, or are of other particular interest or significance.

3.1. Coastal-Continental Clustering Patterns

Interestingly, the three subregions recognized here exhibit a coastal-continental division from the eastern seaboard toward the continental Great Lakes area (Figures 1–3). The MR groups the cold-water-moderated stations from the Canadian maritime provinces and the Gaspe region of Quebec. The CR is the largest subregion geographically, covering northern Ontario and Quebec to upstate New York and northern New England. The SR groups the remaining southern coastal portion of New England and New York, though this subregion contains the most geographic outliers. Several SR stations further inland, including in the northern extents of Ontario and Quebec, are scattered throughout the greater region.

3.2. Long-Term Changes

Figures S1–S12 in Supporting Information S1 are histograms that show seasonal extreme weather event counts per year, with a trend line, based on the LOWESS algorithm using a 20-year window, overlain. These figures have two particular purposes: first, to give a more intuitive overview of trends in extreme weather events, and second, to better understand the later analyses which involve mathematical transforms.

The general trend across all regions and weather variables is the minimal change in the quantity of events through times, in the range of approximately ±2 extreme events between the late 19th century to the early 21st century. The minimal changes, be them positive or negative, in the occurrence of extreme events across each regions' weather stations suggests that there is no strong, consistent long-term pattern in this metric. While there are some locations that exhibit occasional peaks (e.g., rainfall during the spring in the SR in the early 1980s, Figure S7 in Supporting Information S1), these are not part of a broader long-term trend. Instead, the records are characterized more by interannual to interdecadal variation and cyclical patterns at these time scales.

There are some exceptions to the general trend of minimal long-term change. In the MR, there has been a trend over time to gradually been fewer extreme minimum temperature events, most notably during summer and autumn (Figure 4). This trend is most observable at Nepisiguit Falls, NB, which has had approximately 3–4 fewer events over the length of the record. Declines in extreme minimum temperature events since the early 20th century can be observed at many stations across eastern North America (e.g., Drummondville, QC, Indian Lake, NY, and Lewiston, ME during summer, Figures S6 and S10 in Supporting Information S1).

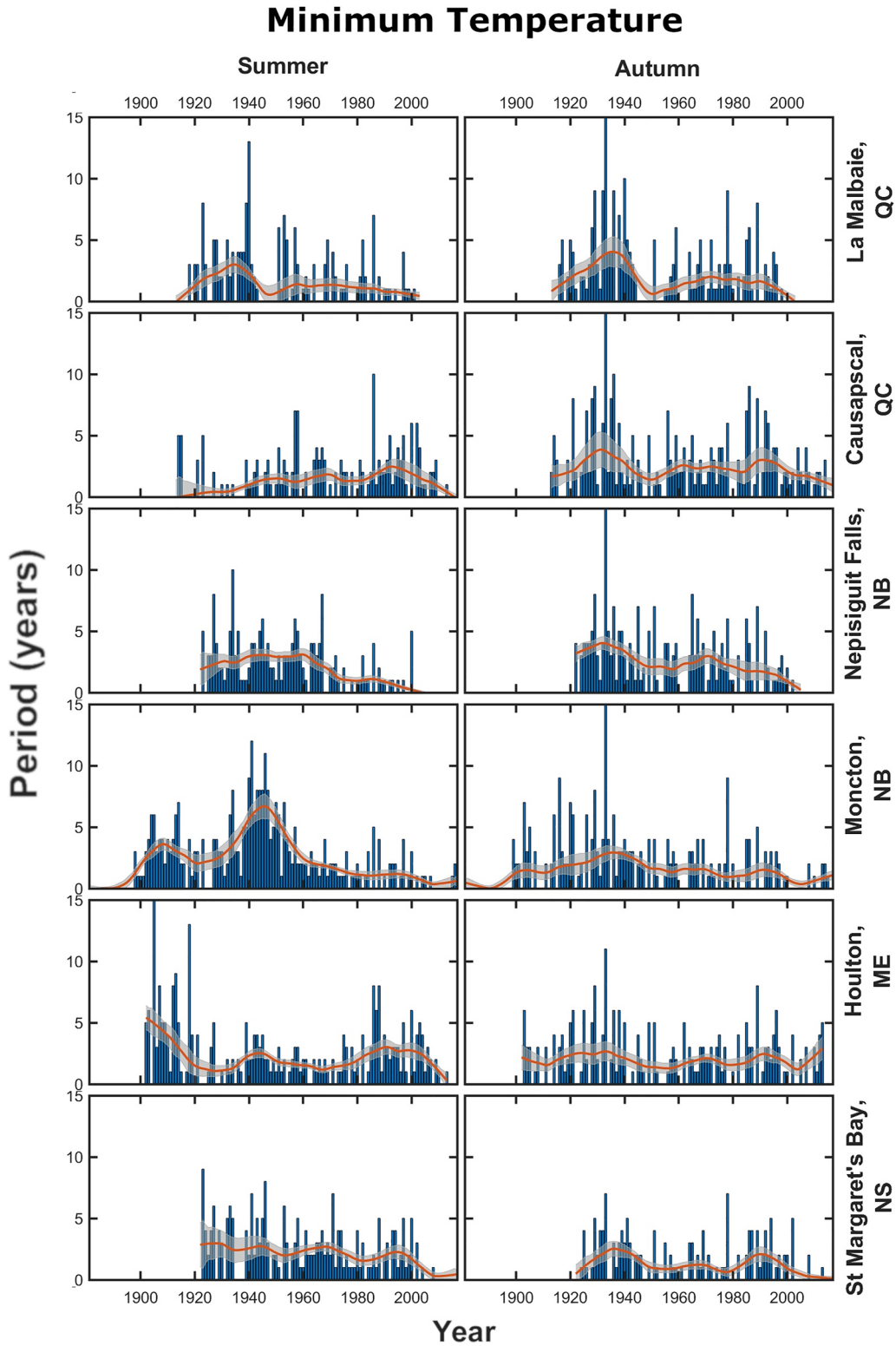

Figure 4. Histograms of extreme minimum temperature events in the Maritime Region, organized by season and station. A trend line is plotted using the Long-term locally weighted linear regressions algorithm for a 20-year rolling window.

Subregional patterns are also present; in the MR, common peaks in extreme minimum temperature are present throughout the subregion in winter (mid-1930s, mid-1990s), spring (late 1930s, 1985–1995), and autumn (mid-1930s, Figure 4 and S2 in Supporting Information S1). Each of the CR and SR exhibits similar subregional patterns in extreme event occurrence (e.g., winter maximum temperature in the CR, ∼1980, Figure S9 in Supporting Information S1; spring extreme rainfall in the SR, early 1980s, Figure S7 in Supporting Information S1).

Extreme precipitation, or lack thereof, appears to be a strongly unifying subregional pattern across eastern North America. The MR and CR are more prone to extreme snowfall in winter, whereas the SR receives very few extreme snowfall events. Conversely, the SR experiences far more winter extreme rainfall events than the two northern subregions (Figures S3–S4, S7–S8, S11–S12 in Supporting Information S1).

3.3. Periodic Patterns and Relations to Climatic Drivers

3.3.1. Schwabe Solar Cycle (SSC)

The strongest observed relationship is with the SSC (Figures S37–S48 in Supporting Information S1). This relationship is the strongest in all regions, and between all weather records, compared to relationships with any other driver. This correlation is visible as a high magnitude area for periods of 9–12 years across all years. Encircled areas are statistically significant at the 95% confidence level. While the SSC is occasionally discontinuous, that is, there are gaps in the 9–12 year periods for some stretches of time, the SSC–extreme weather relationship generally extends across the whole range of the weather records.

An exemplary representation of this relationship is extreme snowfall in the SR (Figure 5, S44 in Supporting Information S1). The temporal recurrence of extreme snowfall events across all seasons is very strongly correlated to the SSC and is generally continuous or nearly continuous.

Extreme winter snowfall in Lewiston is a particularly striking example of a continuous relationship between a weather record and the SSC (Figure 5). Several strong peaks (above the 90% confidence level) ranging from 7.8 to 13.5 years were identified in the spectral periodogram for Lewiston, which occur most strongly from approximately 1910–1950 and again from 1980 to 2010, though weaker, statistically insignificant oscillations in this range also occur during 1950–1980. The XWT results indicate a strong, continuous relationship with the SSC from 1910 to 2010. In contrast, for Plymouth-Kingston, MA extreme snowfall indicates a discontinuity in its relationship with the SSC from approximately 1945–1960. An inspection of its histogram (Figure S8 in Supporting Information S1) indicates few extreme snowfall events occurred during this interval in Plymouth-Kingston. When any wavelet transform is done for null (or nearly null) data, no periodicities will be reported; many wavelet scalograms will show low-magnitude regions at certain years, and this frequent explanation for discontinuities in SSC–extreme weather relationships can be derived by inspection from the extreme weather histograms.

3.3.2. Pacific Decadal Oscillation (PDO)

The next most important relationship for extreme weather records, after the SSC, was the PDO (Figures S49–S60 in Supporting Information S1). This relationship was also strong across all regions but is not as universally present as with the SSC. Figure 6, which shows the correlation between PDO and winter extreme maximum temperature in the MR, as well as the corresponding spectral periodograms and CWT scalograms, encapsulates the various relationships visible for the PDO. In the winter there are significant, albeit discontinuous, correlations between PDO and weather records for 15–25 year periods, in particular in Causapscal, QC (1930–1970s) and Moncton, NB (1920–1980s). Supporting observations can be made in the periodograms. Causapscal has an 18.3 years peak and Moncton has multiple peaks between 19 and 28 years for their respective winter extreme maximum temperature records. The corresponding CWTs shows a similar, significant periodicities for Causapscal and for Moncton for the same time range as when there is a strong correlation to PDO. Similar observations can be made in the summer (Figure S49 in Supporting Information S1). Across the whole of the MR and for all seasons, there is a ∼4–8 years common oscillation between the PDO and extreme maximum temperature events between the 1940 and 1960s. The spectral periodograms for most stations, especially for spring and autumn, have statistically significant peaks (90% confidence level) around 5 years (Figures 6 and S13 in Supporting Information S1). In a similar vein, the CWT show statistically significant periodicity in the 4–8 years range between the 1940 and 1960s (Figures 6 and S25 in Supporting Information S1). It is also notable that 4–8 year periodicity common between 1940 and 1960s is not purely a result of a greater quantity of extreme events at that time, as the

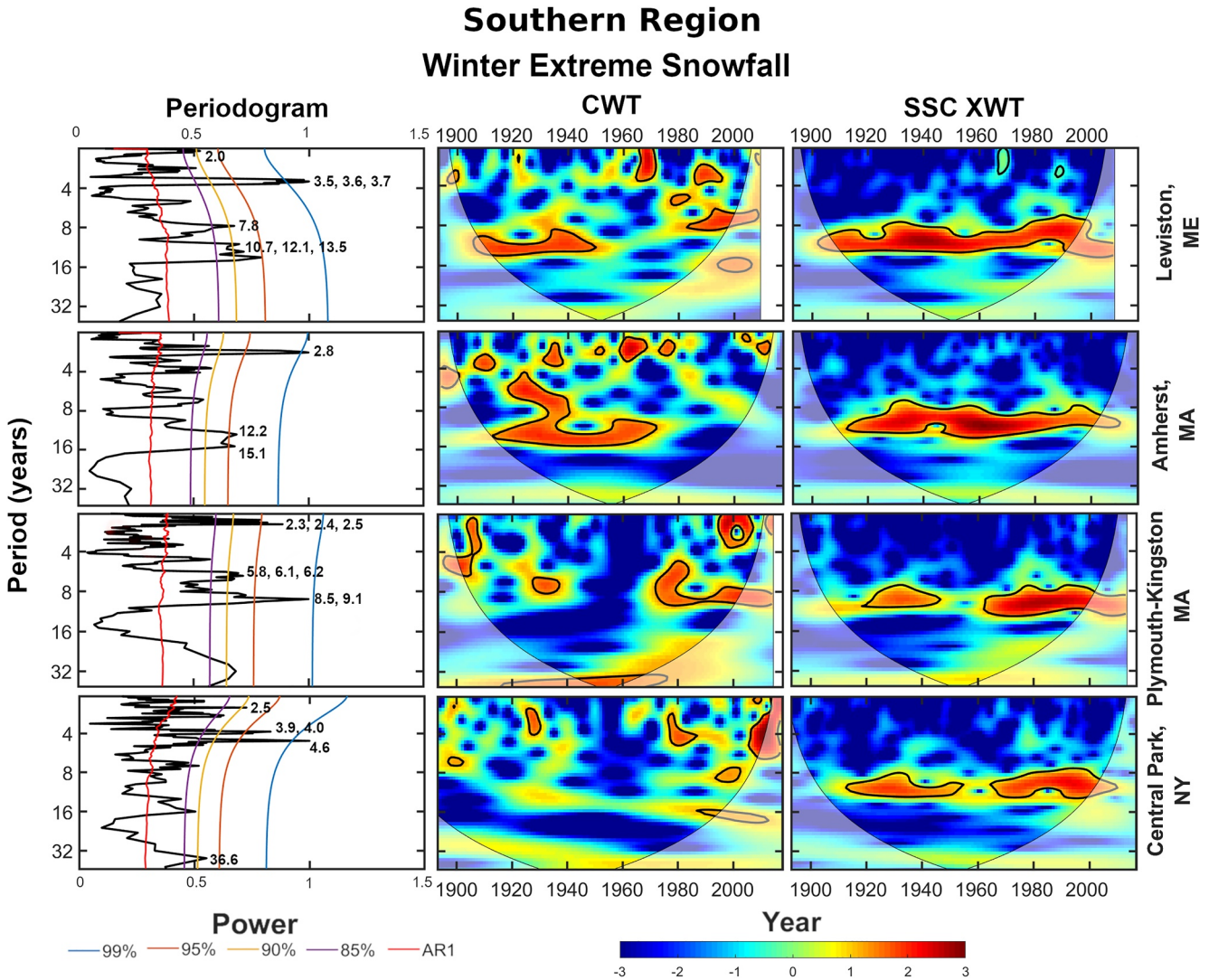

Figure 5. For weather stations in the Southern Region, spectral analysis and continuous wavelet transforms of the winter extreme snowfall records, and cross wavelet transforms of the winter extreme snowfall records and the Schwabe solar cycle. Peaks on the spectral periodograms exceeding the 90% confidence level are labeled with their corresponding cycle length in years.

histograms and the trend line suggest minimal to no long-term changes in the quantity of extreme weather events (Figure S1 in Supporting Information S1).

Similar trends across all locations were recognized for the correlations between PDO and other weather records (Figures S50–S60 in Supporting Information S1). Good examples of strong correlations for the 15–25 year period include most stations, across all regions, for winter extreme temperatures. Such correlations with extreme temperature are often observed in the summer although overall, many occur prior to 1980. Correlations of 15–25 years are typically weaker or absent across all regions in the autumn, as well as during spring in the CR.

The correlations between PDO and precipitation were not as robust as they were with extreme temperatures, though many strong relationships were still prevalent. Examples of the 4–8 year periodicity were more commonly observed than those of the 15–25 year periodicity, in particular for extreme snowfall in the MR (Figure S52 in Supporting Information S1) and CR (Figure S60 in Supporting Information S1). Nepisiguit Falls (MR) and Belleville, ON (CR) are excellent examples of significant correlations for extreme snowfall events, across all seasons, to the 4–8 years PDO periodicity in the 1940–1960s.

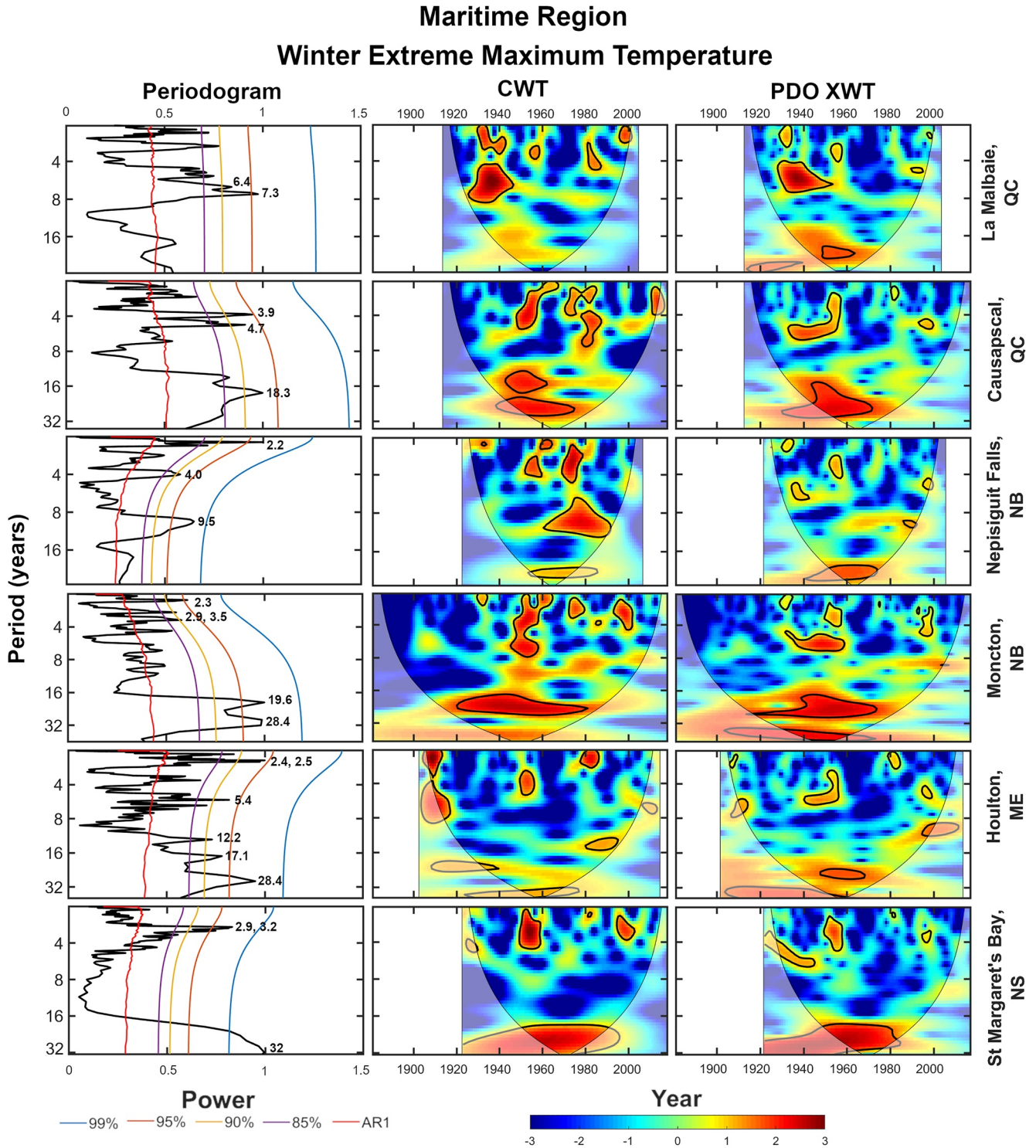

Figure 6. For weather stations in the Maritime Region, spectral analysis and continuous wavelet transforms of the winter extreme maximum temperature records, and cross wavelet transforms of the winter extreme maximum temperature records and the Pacific Decadal Oscillation. Peaks on the spectral periodograms exceeding the 90% confidence level are labeled with their corresponding cycle length in years.

Other notable correlations of longer common oscillations with the PDO (30+ years) are exhibited by stations with the longest running weather records. For example, Central Park's record begins in 1869; because of its length, longer common oscillations can be recognized. Here, another mode of the PDO exhibits a relationship with Central Park extreme rainfall, particularly in the spring and summer (Figure S55 in Supporting Information S1).

3.3.3. Quasi-Biennial Oscillation (QBO)

The QBO was another significant regional driver of climate. It is characterized by intermittent correlations with 2.1–2.5 year periods throughout eastern North America. Unlike other climate oscillations, QBO has a marginally more significant influence on extreme precipitation rather than extreme temperatures. Consider Figures 7 and S71 in Supporting Information S1, which show XWT results between extreme rainfall in the CR and the QBO. Most stations in the CR show some areas with statistically significant correlations of 2–3 year periods across all seasons. The results for the summer, however, are particularly instructive. Comparing to the periodogram for rainfall in the CR (Figure S23 in Supporting Information S1), all stations but Belleville, ON have strong peaks between 2.0 and 2.5 years, which can be attributed to the QBO. Also of note in the summer is the presence of an 8–20 years cyclicity prior to ∼1980, which is most strongly exhibited in Woodstock, ON. This result is likely caused by an interaction of the QBO with the SSC between the 1950 and 1980s.

The other regions bear similar results (Figures S61–S72 in Supporting Information S1). Extreme precipitation generally exhibits marginally stronger relationships with QBO, compared to extreme temperature. The effect of the QBO on extreme maximum temperature is generally strongest in the winter and weakest in the summer in each region; however, the effect of the QBO on extreme minimum temperature is largely seasonally invariant. The 8–20 cycle associated with QBO–SSC interaction is most strongly expressed with extreme precipitation, particularly in the MR Figures S63–S64 in Supporting Information S1; however, spring extreme maximum temperature consistently shows this relationship across all regions (Figures S61, S65, S69 in Supporting Information S1).

3.3.4. El Niño Southern Oscillation (ENSO), Arctic Oscillation (AO), and North Atlantic Oscillation (NAO)

ENSO (Figures S73–S84 in Supporting Information S1), AO (Figures S85–S96 in Supporting Information S1), and NAO (Figures S97–S108 in Supporting Information S1) were not observed to be strong drivers of climate in Eastern North America, in comparison to PDO and QBO. When there is a correlation between these drivers and a weather record, it is usually highly discontinuous, and is characterized by a brief time window of correlation and a longer time window lacking correlation. When a correlation is present though, it is generally significant. There are no prominent seasonal or regional variations in the importance of these drivers.

When a correlation between one of these three drivers is observed with a weather record, correlations with similar periodicities at similar time intervals are also frequently observed with the two other drivers. A particularly striking example of this effect is seen with spring extreme minimum temperatures in the CR (Figure 8). The periodograms show similar, well-defined peaks for all stations in the spring, having periods ranging from 5.0 to 6.2 years. The corresponding XWT plots for ENSO, AO, and NAO all show, in the time window spanning 1930–1960, significant correlations at the requisite periodicity to the spring extreme minimum temperature records. These correlations are particularly pronounced for ENSO and AO as they are seen for every station. For NAO, these correlations are similarly seen for Kapuskasing and Amos, but are bit more limited with respect to the temporal range at the four remaining stations, although these correlations remain statistically significant at 95%. This interrelation between ENSO, AO, and NAO is broadly observed across all extreme weather variables, regions, and seasons, where correlations are found. Additionally, while the trend of less-pronounced correlation for NAO is also broadly observable, there appears to be a slight spatial gradient where the influence of both the NAO and AO increases with latitude.

3.3.5. Atlantic Multidecadal Oscillation (AMO)

The AMO is the least influential extreme weather driver investigated (Figures S109–S120 in Supporting Information S1). Despite that, it is of significance because its influence follows a clear spatial gradient across eastern North America, unlike the other drivers tested (Figures 9–11). For extreme maximum temperature in the MR (Figure 9), there is statistically significant (95% confidence level) correlation between the AMO signal and the weather record in the winter for St. Margaret's Bay—a coastal station—with a generally stationary common period of 20–30 years. Other stations have correlations with a similar magnitude, time frame, and period range

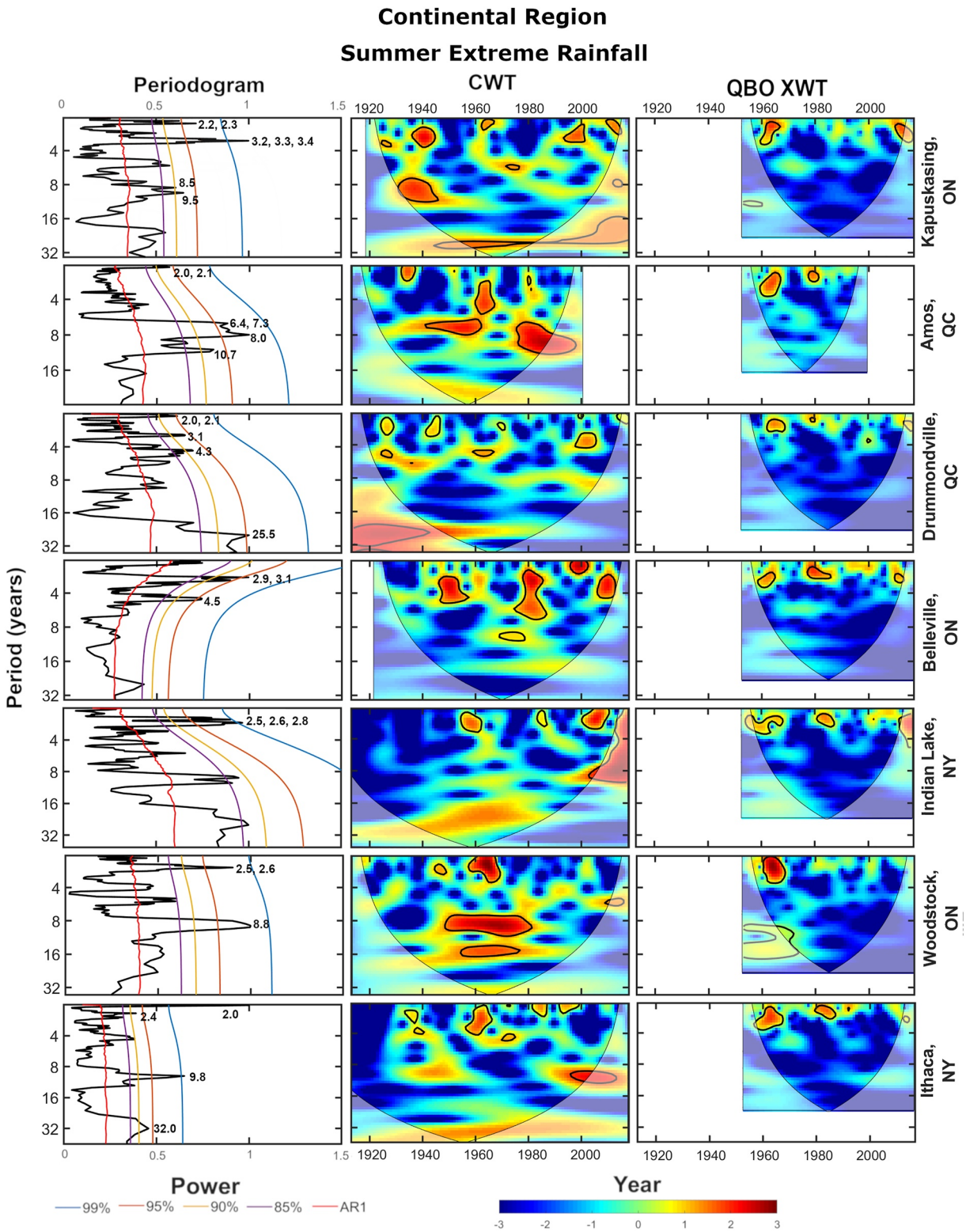

Figure 7. For weather stations in the Continental Region, spectral analysis and continuous wavelet transforms of the summer extreme rainfall records, and cross wavelet transforms of the summer extreme rainfall records and the Quasi-Biennial Oscillation. Peaks on the spectral periodograms exceeding the 90% confidence level are labeled with their corresponding cycle length in years.

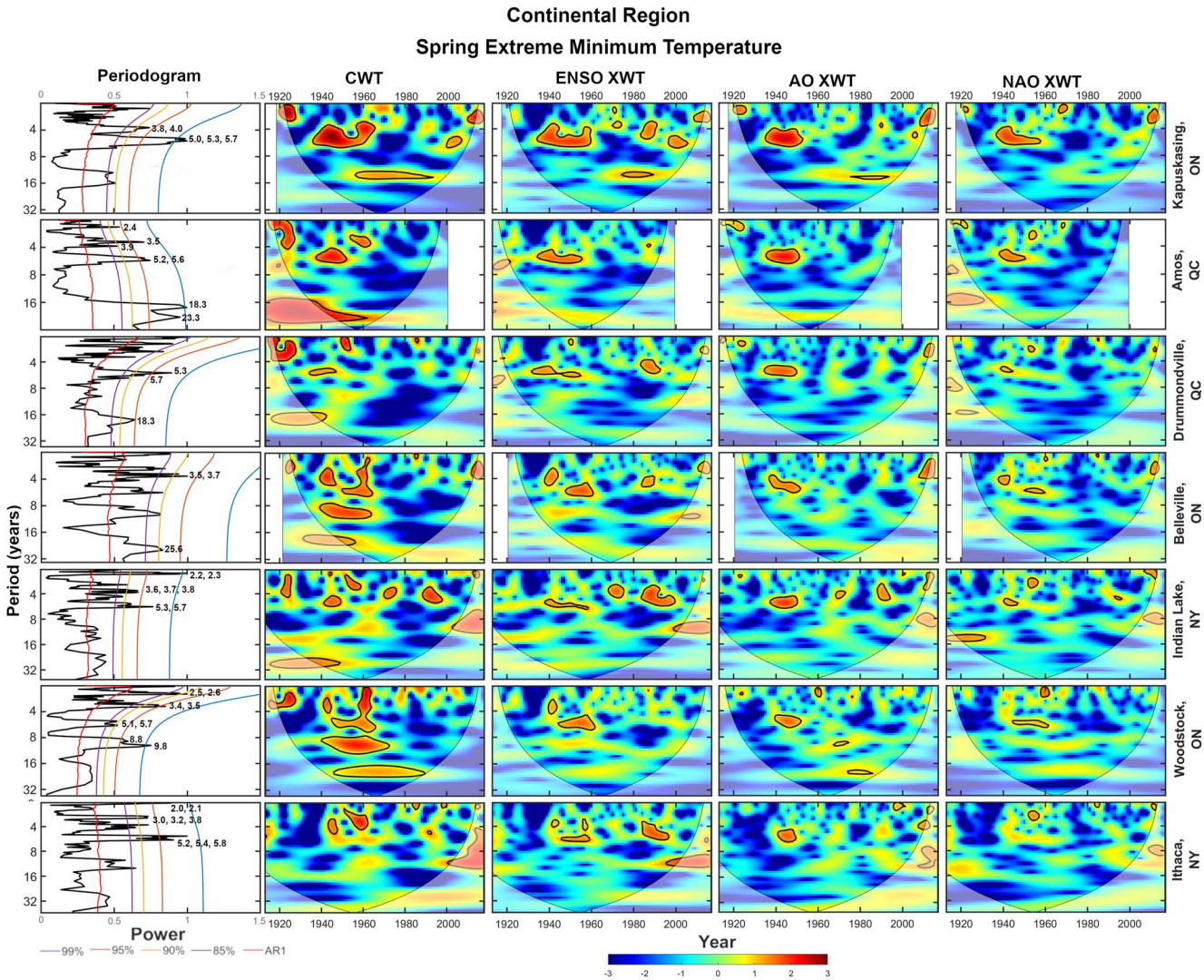

Figure 8. For weather stations in the Continental Region, spectral analysis and continuous wavelet transforms of the spring extreme minimum temperature records, and cross wavelet transforms of the spring extreme minimum temperature records and each of the El Niño Southern Oscillation, Arctic Oscillation, and North Atlantic Oscillation. Peaks on the spectral periodograms exceeding the 90% confidence level are labeled with their corresponding cycle length in years.

in the XWT plot, primarily in the winter and summer, albeit these are not significant at 95% (Figures 9 and S109 in Supporting Information S1). Note that the AMO is characterized by its typical band (50–90 years) and subharmonics (16–24 years), and while there are other, higher frequency significant correlations, these may be related to interactions between the AMO and other climatic drivers.

In the SR the effects of the AMO are similar to what was observed in the MR, particularly in the winter (Figure 10) and summer (Figure S113 in Supporting Information S1), although rarely at a statistically significant level. Of note are the relationships exhibited in Central Park, NY. As this is a particularly long record (1869–2017), at the base of the 50–90 years mode of the AMO was observed in each season and is statistically significant (95%) in the summer from approximately 1940–2005.

In contrast, stations in the CR (Figure 11 and S117 in Supporting Information S1) show weak relationships with the AMO, indicating a trend of decreasing importance of AMO further from the Atlantic Ocean. An exception to this is the spring record for Ithaca, which has a statistically significant region, which corresponds well to three peaks on relevant periodogram (Figure S21 in Supporting Information S1) that range from 21 to 32 years, all significant at the 99% confidence level.

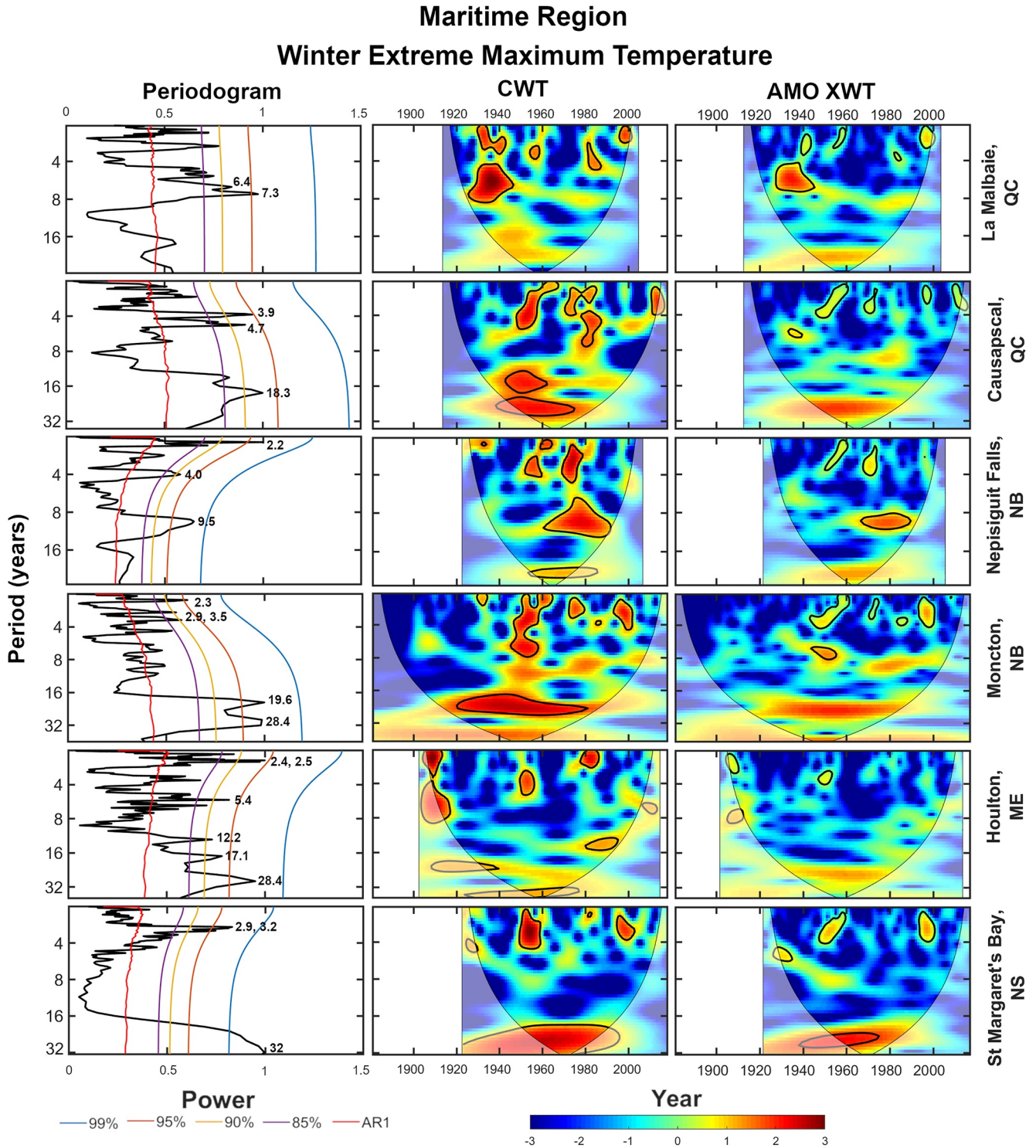

Figure 9. For weather stations in the Maritime Region, spectral analysis and continuous wavelet transforms of the winter extreme maximum temperature records, and cross wavelet transforms of the winter extreme maximum temperature records and the Atlantic Multidecadal Oscillation. Peaks on the spectral periodograms exceeding the 90% confidence level are labeled with their corresponding cycle length in years.

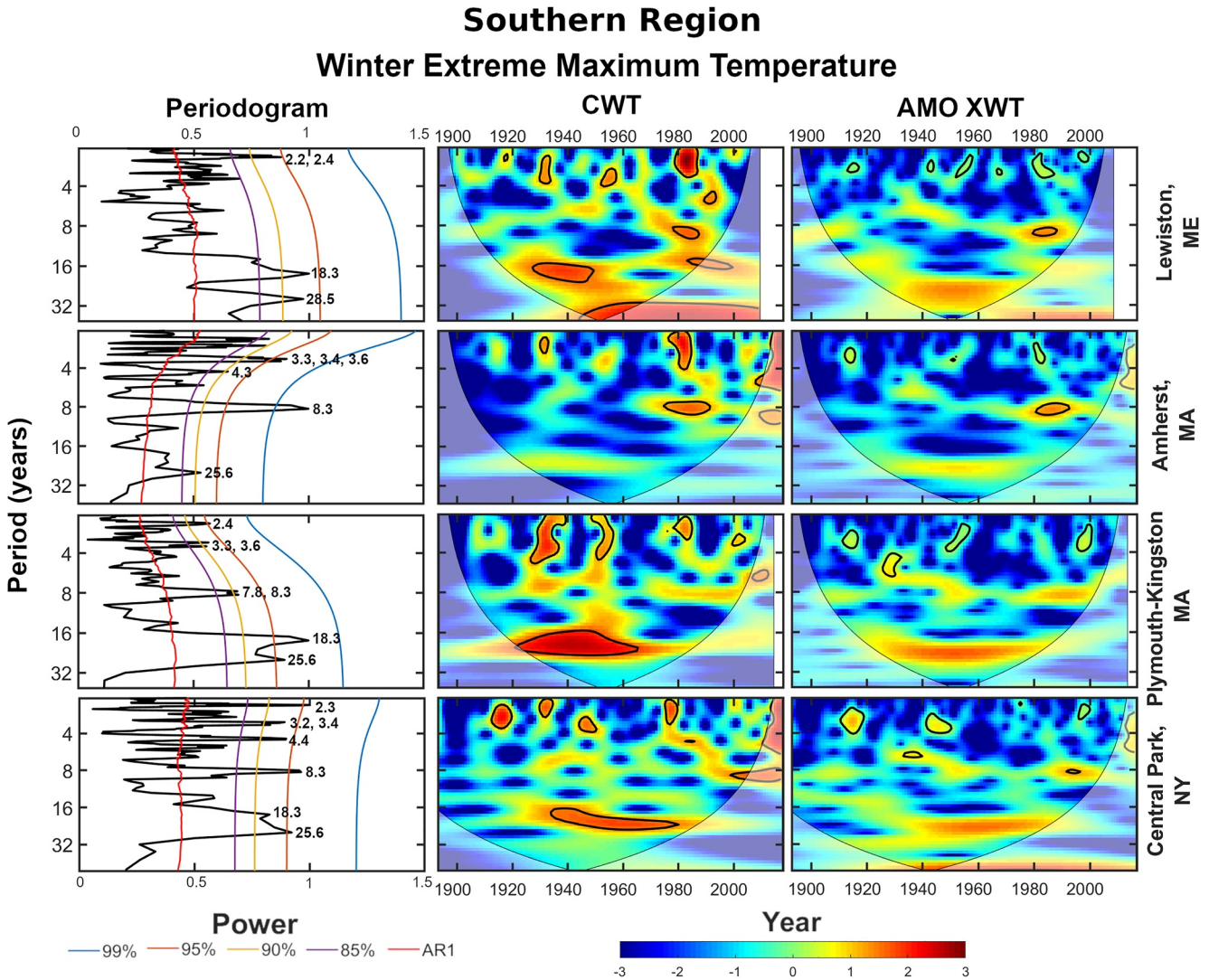

Figure 10. For weather stations in the Southern Region, spectral analysis and continuous wavelet transforms of the winter extreme maximum temperature records, and cross wavelet transforms of the winter extreme maximum temperature records and the Atlantic Multidecadal Oscillation. Peaks on the spectral periodograms exceeding the 90% confidence level are labeled with their corresponding cycle length in years.

Extreme precipitation records also exhibit a similar spatial trend, but the AMO–extreme precipitation correlations are generally not statistically significant except for the 50–90 years mode, which is once again present in common in Central Park for extreme summer rainfall (Figures S111–S112, S115–S116, S119–S120 in Supporting Information S1).

4. Discussion

The subdivision of eastern North America (Figures 1 and 2) into three coastal-continental oriented subregions differs somewhat from typical climate zones, which often follow latitudinal arrangements (e.g., Cui et al. (2021); Gardner et al. (2020); Zhang et al. (2017)) However, instead of using absolute climate data, such as local temperatures, these subdivisions were derived using extreme weather event counts (outlined in Section 2.1), which are relative data. As a weather event is defined as extreme based on the 95th percentile method, latitudinal bias is lowered, and the region can be subdivided based on other natural patterns.

For this region, the natural divisions suggested northern and southern ocean-dominated regions (the MR and the SR, respectively), and an inland region (the CR). This coastal-continental gradient suggests some differences in

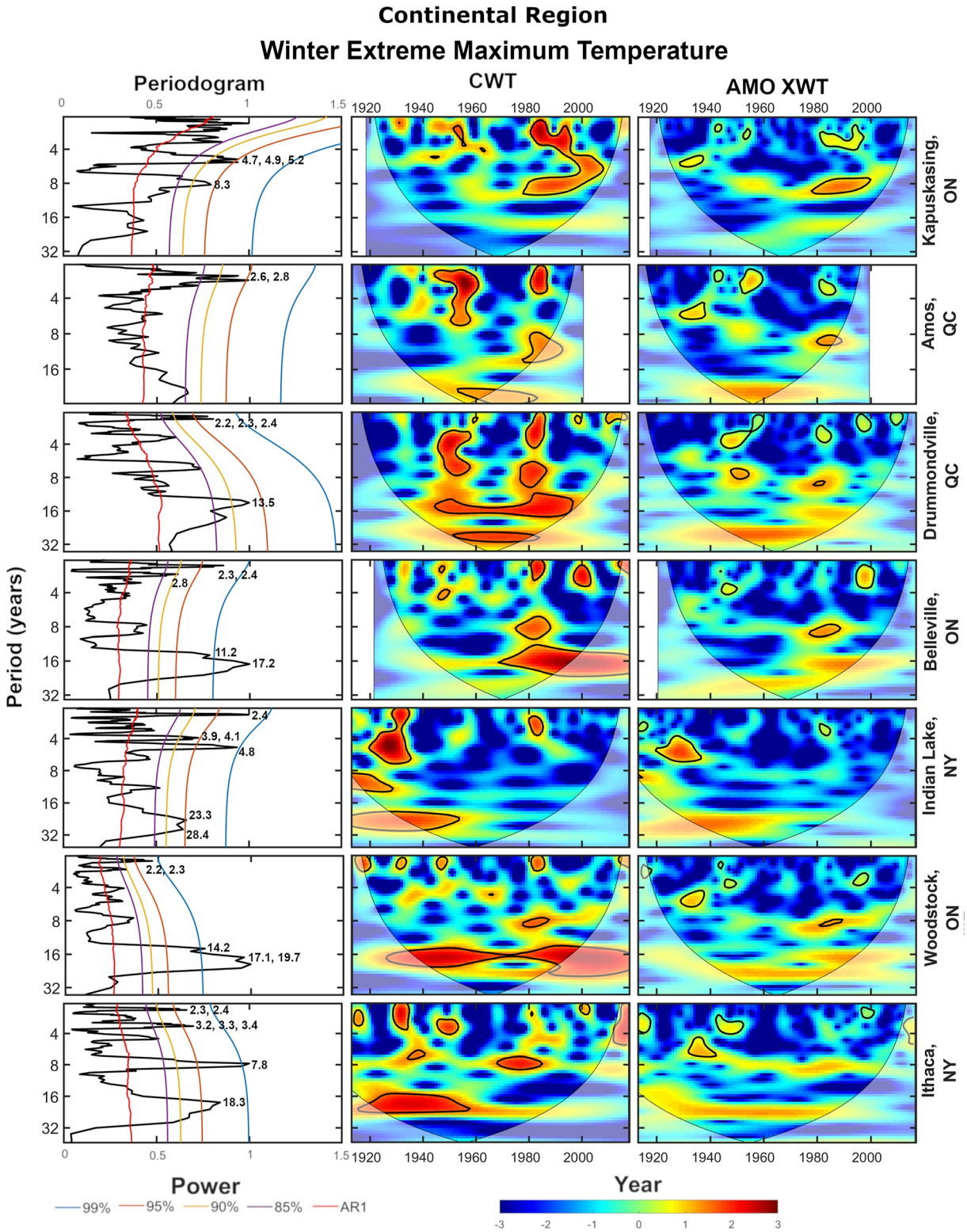

Figure 11. For weather stations in the Continental Region, spectral analysis and continuous wavelet transforms of the winter extreme maximum temperature records, and cross wavelet transforms of the winter extreme maximum temperature records and the Atlantic Multidecadal Oscillation. Peaks on the spectral periodograms exceeding the 90% confidence level are labeled with their corresponding cycle length in years.

each subregion's propensity for extreme precipitation events. Much of the SR is less likely to experience extreme snowfall than either of the MR of CR, whereas the northern MR and CR stations experience fewer extreme rain events, overall. These differences are likely an effect of latitudinal differences.

The SR is also the least centralized group, with several stations scattered throughout the CR. The northern, decentralized SR stations are largely outliers in the region; while they cluster most closely in the SR, these stations can each be found on one branch of the cluster dendrogram, whereas the southern coastal stations can be found on another Figure 2. One possible explanation of the similarities in extreme weather between the outlying stations and the centralized stations of the SR is the proximity of several outlying stations to large water bodies. Particularly for the northwest outliers, stations can be found close to large water bodies, such as Lake Nipissing (Sturgeon Falls, ON) and Lake Kipawa (Kipawa Laniel, QC), which could provide a moderating effect on extreme weather. The northeastern stations of the SR are not located on large waterways, though the topography of region transitions from the St. Lawrence Lowlands toward the sub-mountainous region of the Appalachian Mountain Chain. The transition in topography could contribute to the extreme weather events that occur in this area.

The extreme temperature records across eastern North America do not appear to suggest any subregion is more or less extreme than the others, as stations in each subregion have similar overall occurrences of extreme events. Instead, locations within each subregion appear to experience similar timing of extreme events; the sample stations within each subregion displayed comparable long-term trends and comparable peaks and troughs, suggesting that coastal-continental groupings largely influence the temporal distribution of extreme events, and not their quantity.

4.1. Extreme Weather Primarily Driven by Climate Oscillations

The occurrence of extreme weather events in eastern North America is primarily mediated by a variety of climate oscillations. Four broad observations are noted as follows:

1. The SSC is by far the most significant driver of climate across all regions.
2. The PDO and QBO are also important drivers, but they are secondary to the SSC.
3. The El-Niño Southern Oscillation (ENSO), NAO, and AO are tertiary drivers and appear interrelated.
4. The AMO has the weakest correlation to any of the weather records of all climatic drivers tested, but it has the clear spatial gradient as it is most significant nearer to the coast.

The SSC was shown to be the dominant climatic driver of extreme weather events in eastern North America. Compared to the six other drivers tested, the SSC exhibited long-standing, stationary relationships with all extreme temperature and precipitation records across all regions studied, and accounts for many of the quasi-decadal periodicities observed in spectral and CWT analyses. The strength of the interaction between the SSC and extreme weather across all three regions parallels that reported elsewhere in North America (Currie, 1993; Currie & O'Brien, 1988; Mendoza et al., 2001; Vines, 1977; Vines, 1984; Walsh & Patterson, 2022) and globally (Currie & Vines, 1996; Du et al., 2017; Laurenz et al., 2019; Lockwood, 2012; Maliniemi et al., 2014; Meehl & Arblaster, 2009; Meehl et al., 2009; Sfîcă et al., 2018; van Loon & Shea, 1999; van Loon et al., 2004; Vines, 1977, 1980), though much of the literature does not discuss this relationship in reference to extreme weather, but rather in regards to average climate records.

The influence of the SSC is so widespread and strong due to the fundamental linkage of solar radiation and climate. As solar flux drives atmospheric, oceanic, and terrestrial heating, factors affecting solar flux are the primary drivers of Earth's climate variations on both the long- and short-term (Kopp, 2014). The SSC is characterized by the number of sunspots on the sun's surface, which shares a direct relationship with solar flux (Yang et al., 2010). Thus, the impact of the SSC on global and regional climate and extreme weather is not unprecedented, though the recognition of the SSC–extreme weather relationship has not been well-documented.

Many of the low-interdecadal oscillations seen in periodograms and CWT plots were attributed to the PDO using XWT analysis. Regional relationships of the interannual and interdecadal oscillations of the PDO were particularly prevalent with both temperature extremes before ~1970, indicating that the PDO was a significant driver of extreme temperatures before this time. This change could be related to the 1977 regime shift in the Pacific Ocean, which is characterized by a strong and sudden change in sea-level pressure and temperature, shifting from PDO- to PDO+ (Ebbesmeyer et al., 1990; Hare & Mantua, 2000; Mantua & Hare, 2002; Trenberth, 1990). This regime shift appears to be correlated to the weakened relationship that PDO has with extreme weather after 1980. Other

Pacific regime shifts, such as those occurring in the 1920, 1940, and 1980s (Hare & Mantua, 2000; Mantua & Hare, 2002; Minobe, 1999), did not appear strongly when relating extreme weather and the PDO, though the late 1940s regime shift could have been related to the diminishing PDO–extreme minimum temperature relationship in some MR stations after ∼1945 (Figure S50 in Supporting Information S1).

While the regime shifts may explain the sudden change in the PDO–extreme weather relationships, this does not explain the prolonged disconnection between PDO and extreme weather after the 1977 regime shift. One consideration is the link between the PDO and other climate oscillations. Many climate oscillations are known to interact with one another depending on their respective phases, resulting in modulation or (de)amplification of one or both oscillations (e.g., Valdés-Pineda et al. (2018), Zhang et al. (2020)). It is possible that the influence of the PDO on eastern North American extreme weather may have been amplified or deamplified by interactions with other climate oscillation during the early 1900s to ∼1980 or 1980 onward, respectively. Exploring the possibility of PDO interactions and their effects on eastern North American extreme weather is beyond the scope of this study, but could be an avenue of future research.

While the climatic effects of the PDO are more commonly associated with western North America, links to droughts, temperatures, and other environmental factors have been previously found for eastern North America as well (B. Bonsal et al., 2001; B. R. Bonsal et al., 2001; Goodrich & Walker, 2011; Kuss & Gurdak, 2014; Le Goff et al., 2007; Nigam et al., 1999; Rodionov & Assel, 2003; Tan et al., 2016). The 50–70 years band of the PDO has also been attested to drive climate in North America (Labat, 2008; Nalley et al., 2019), but the instrumental data record for eastern North America is too brief to robustly assess whether that band drives regional extreme weather. Furthermore, the PDO also indicated oscillatory relationships with both temperature and precipitation extremes on shorter time-scales (e.g., 4–8 years). The PDO exhibits several oscillatory modes (Juanxiong et al., 2004); the interannual mode of the PDO, while not as strong as its interdecadal and multidecadal modes, is prevalent throughout its record. This interannual mode is largely a result of the relationship between the PDO and ENSO; the PDO while occurring in the North Pacific, is thought to be an amalgamation of several influences, with the ENSO being a primary influence (Newman et al., 2003, 2016; Rao et al., 2019).

The QBO has a strong but intermittent correlation in its 2–3 years band with extreme weather across all regions, particularly with extreme precipitation. The existing body of literature, while limited, suggests the presence of similar oscillations attributable to the QBO in precipitation and temperature-related variables on local and global scales (Baldwin et al., 2001; Chattopadhyay & Bhatla, 2002; Gray et al., 2018; Lau & Sheu, 1988; Patterson & Swindles, 2015). The mechanisms of this influence lie in the impact the QBO has on the Arctic polar vortex. The QBO is characterized by the oscillation of equatorial stratospheric easterly and westerly winds, which propagate poleward by extratropical planetary waves; the negative, easterly phase of the QBO weakens and destabilizes the polar vortex, whereas to positive, westerly phase of the QBO strengthens the polar vortex (Anstey & Shepherd, 2014; Boer & Hamilton, 2008; Holton & Tan, 1980). In turn, the strength and stability of the Arctic polar vortex greatly impact Northern Hemisphere temperature and precipitation variation by determining the flow pattern exhibited by the polar jet stream (zonal versus. meridional flow). The flow pattern impacts the position of warm and cold air masses, as well as storm tracks and their ensuing precipitation (Walter & Graf, 2005). In particular, instances of weak and unstable polar vortices are noted to be related to instances of extreme temperature and precipitation (Huang et al., 2021; Overland & Wang, 2019; Overland et al., 2020).

The intermittent nature of the QBO–extreme weather connection is likely due to the strength of the QBO shifts and the interaction in atmospheric processes, such as extratropical planetary waves or other climate oscillations. The interaction of other atmospheric processes, both oscillatory and non-oscillatory, may overprint or obscure the QBO–extreme weather relationship (e.g., weakening of planetary wave propagation, thus weakening the QBO–polar vortex connection). Furthermore, other climate oscillations, namely the AO and NAO, impact the variability of the Arctic polar vortex (Baldwin & Dunkerton, 1999; Walter & Graf, 2005); their influence on the dynamic changes the polar vortex experiences may obscure the influence the QBO has at a given point in time.

Similarly, other climate oscillations can interact with the QBO, modifying its impact on eastern North American extreme weather. For example, the incidence of longer interdecadal relationships between the QBO and many of the extreme weather records prior to ∼1980 can be attributed to a modulatory effect of the SSC on the QBO (Fischer & Tung, 2008; Hamilton, 2002; Quiroz, 1981).

Similar moderate relationships between extreme weather and ENSO, AO, and NAO were observed across eastern North America. The existing body of literature also suggests these oscillations as drivers of eastern North America climate, although ENSO (Fuentes-Franco et al., 2016; Hu & Feng, 2012; Ropelewski & Halpert, 1986; Toniazzo & Scaife, 2006) is generally considered separate from AO and NAO (D'Arrigo et al., 2003; Li et al., 2017; Nalley et al., 2013, 2012; Patterson & Swindles, 2015; Thompson & Wallace, 1998; Wang et al., 2005; Zhao et al., 2013). The latter two drivers are often considered together, as the NAO is considered to be a subset of AO (Ambaum et al., 2001; Patterson & Swindles, 2015; Rogers & McHugh, 2002). The results have suggested broad similarities between the effects of ENSO, AO, and NAO on extreme weather, although with NAO playing a slightly smaller role, through both the AO and NAO exhibited noticeably stronger influences on higher latitude stations. As the NAO and AO originate at high latitudes, this observation is coherent. The similarity between the ENSO, AO, and NAO results are possibly due to the similarity in periodicities that characterize the three oscillations. Given the discontinuous nature of the correlations, it is possible that all three oscillations amplify each other, and will thus have a greater effect on climate together at certain points in time. The interaction between these oscillations has been explored, suggesting that they can impact eastern North America both individually, and interactively. Particularly, when ENSO is positive (negative) and AO/NAO are negative (positive), the effects of these oscillations are amplified (reduced). In the Northern Hemisphere, ENSO+ and AO/NAO- typically result in greater precipitation and cold temperature anomalies, whereas ENSO- and AO/NAO + result in more warm temperature anomalies (Lim & Schubert, 2011; Seager et al., 2010; Zhang et al., 2019).

The AMO indicated the weakest influence across eastern North America, but a clear spatial gradient was observed with greater influence near the Atlantic Ocean. The strongest effect was observed with extreme temperatures. The coastal stations of the MR and SR were most influenced by the AMO. The influence of the AMO was more subdued in the CR. The AMO is defined by cyclicity in the circulation of warm and cool Atlantic surface waters. Thus, it follows that stations nearest to these waters would stand to be highly influenced by such an oscillation, whereas more inland stations would be characterized by diminished effects.

While the AMO is considered to have a characteristic 64 year period—something that is not easily characterizable with available instrumental records and has only been observed in this study for the long-running record in Central Park, NY—16–24 years subharmonics are also known to exist (Knudsen et al., 2011; Patterson & Swindles, 2015; Ruiz-Barradas et al., 2013). These subharmonics are weakly observed across eastern North America—particularly in the MR and SR—in the mid-20th century. It is possible that the characteristic period of the AMO is influential to long-term extreme weather variability, however, this study is limited by the availability of instrumental climate data, which, with the exception of Central Park, often does not cover a long enough time frame to fully characterize any potential relationship.

Also of note are the smaller, intermittent correlations in the XWTs that correspond to shorter periods, usually interannual. The AMO is thought to interact with other oscillations, particularly the PDO and ENSO (Goly & Teegavarapu, 2014; McCabe et al., 2004; Wang et al., 2018). At some times, such as in the 1950 and 1960s, there appear to be similarities between correlations with weather records and both AMO, ENSO, and PDO (e.g., CR, autumn maximum temperature, Figures 11, S57, S81 in Supporting Information S1). The interactions between the AMO and other oscillations potentially explain the nature of these interannual AMO–extreme weather correlations, though further analysis on the connections between these oscillations, their phases, and their relationships to regional extreme weather is needed to characterize the combined effects on eastern North America. Exploring these AMO connections would also provide insights to the separability of the interdecadal AMO mode and the interdecadal PDO mode, both of which are recognized to some degree in their respective XWTs, though with different spatio-temporal patterns.

4.2. Negligible Long-Term Trends in Extreme Weather

Many of the seasonal extreme weather records across eastern North America indicated negligible long-term trends. For most cases, there was no increase or decrease in extreme weather events between the early 20th century to the early 21st century. The primary exception to this trend was seen in extreme minimum temperature. Across all three regions, weak decreases in events during summer were often observed. Within eastern North America, literature suggests that average minimum daily temperatures have increased substantially since the beginning on the 20th century (Ahmed et al., 2014; B. Bonsal et al., 2001; B. R. Bonsal et al., 2001; Nalley

et al., 2013; Vincent et al., 2018; Yagouti et al., 2008; Zhang et al., 2000). The increase in minimum temperatures allows for fewer extremes over time.

A secondary consideration for this slight decrease in extreme minimum temperature events is an increase in atmospheric moisture levels. Other studies for eastern North America have suggested an increase in annual precipitation (Assani et al., 2012; B. Bonsal et al., 2001; B. R. Bonsal et al., 2001; Deng et al., 2016; Gan, 1995; Groisman & Easterling, 1994; Mekis & Vincent, 2011; Shephard et al., 2014; Walsh & Patterson, 2022; Zhang et al., 2001). Note that this study does not suggest an increase in extreme precipitation events, which means that total precipitation is not influenced by extreme events, which agrees with Zhang et al. (2001), who suggest that increases in precipitation are attributable to an increase in small to moderate precipitation events. With higher humidity, daily minimum temperatures become more moderated, resulting in fewer cases considered extreme. Alternatively, given that the decrease in extreme events is only observed for minimum temperature and not maximum temperature, an explanation similar to that for precipitation is also valid, where increases in average maximum and minimum temperature are not heavily influenced by extreme events, but by small to moderate events.

5. Conclusions

Extreme maximum and minimum temperature, rainfall, and snowfall events were extracted from instrumental weather records from across eastern North America. These extreme weather records were used to subdivide the region into subregions using agglomerative hierarchical clustering. Three clusters were identified based on similarities in the extreme weather records from 90 stations across eastern North America. Extreme weather records from exemplary stations from each subregion were analyzed using time series analysis techniques, namely LOWESS regression, spectral analysis, CWTs, and cross wavelet transforms against time series of known climatic drivers, to characterize long-term and periodic trends in regional extreme weather. While long-term increases or decreases in extreme weather events are not strongly characteristic of the region, with exception to a small general trend of a decrease in extreme minimum temperature events, the occurrence of these events is highly cyclic and well-correlated to a variety of climatic drivers. The strongest correlation observed was with the SSC, which represented the most continuous, long-term relationship of the drivers tested. PDO and QBO were also important drivers, but they were broadly discontinuous, and not as characteristically omnipresent at the SSC. The El Niño-Southern Oscillation (ENSO), NAO, and AO were occasionally important in driving climate in the region, but more importantly, they showed a close interrelation as the time-frequency correlations to the extreme weather records were largely common between the three drivers. Finally, the AMO was shown to have the least effect on regional extreme weather, but unlike the other drivers tested, it had a clear spatial gradient where its influence was most important closer to the Atlantic Ocean. A secondary outcome of this study was a systematic time series analysis characterization of 17 weather stations in eastern North America, the results of which are available in the supplementary material (Figures S1–S120 in Supporting Information S1).

The interactions between the various climatic drivers tested were demonstrated to have an impact on extreme weather. Two interactions of note include the one between the ENSO, NAO, and AO, as well as a likely interaction between the QBO and SSC observed for records prior to 1980. The results of this study indicate the importance of various combinations of the seven studied oscillations on the occurrence of extreme weather. This suggests that analysis of the impact of additional cyclic climate phenomena, including major global ones, on the occurrence of extreme weather events would be a fruitful line of research. Furthermore, the natural division of eastern North America by the similarities in relative extreme weather events poses potential for better regional understanding of extreme weather. Such a methodological approach could be applied in different regions of a similar scale to better inform key regional stakeholders of the typical trends in extreme weather.

Acronyms

SSC	Schwabe Solar Cycle
AMO	Atlantic Multidecadal Oscillation
PDO	Pacific Decadal Oscillation
NAO	North Atlantic Oscillation
AO	Arctic Oscillation
ENSO	El Niño Southern Oscillation
QBO	Quasi-Biennial Oscillation

Data Availability Statement

Climate data for Canadian climate stations was obstained from Environment and Climate Change Canada (Environment and Climate Change Canada, 2020). United States climate station data was obtained from the National Oceanic and Atmospheric Administration (National Oceanic and Atmospheric Association, 2020). Data for the climate oscillations used, Schwabe Solar Cycle, Pacific Decadal Oscillation, Atlantic Multidecadal Oscillation, North Atlantic Oscillation, Arctic Oscillation, El Niño Southern Oscillation, and Quasi–Biennial Oscillation, was obtained from SILSO (2021), Deser et al. (2016), Trenberth et al. (2021), Hurrell and NCAR (2020), NCAR (2020), Trenberth and NCAR. (2020) and NCAR (2013), respectively. All data is freely available to the public.

Acknowledgments
This research was supported by a Natural Sciences and Engineering Research Council of Canada Discovery grant to RTP.

References

Ahmed, S. I., Rudra, R., Dickinson, W. T., & Ahmed, M. (2014). Trend and periodicity of temperature time series in Ontario. *American Journal of Climate Change*, *3*(03), 272–288. https://doi.org/10.4236/ajcc.2014.33026

Alexander, M. A., Kilbourne, K. H., & Nye, J. A. (2014). Climate variability during warm and cold phases of the Atlantic Multidecadal Oscillation (AMO) 1871–2008. *Journal of Marine Systems*, *133*, 14–26. https://doi.org/10.1016/j.jmarsys.2013.07.017

Allen, S. M., Gough, W. A., & Mohsin, T. (2015). Changes in the frequency of extreme temperature records for Toronto, Ontario, Canada. *Theoretical and Applied Climatology*, *119*(3–4), 481–491. https://doi.org/10.1007/s00704-014-1131-1

Ambaum, M. H., Hoskins, B. J., & Stephenson, D. B. (2001). Arctic oscillation or North Atlantic oscillation? *Journal of Climate*, *14*(16), 3495–3507. https://doi.org/10.1175/1520-0442(2001)014<3495:aoonao>2.0.co;2

Anstey, J. A., & Shepherd, T. G. (2014). High-latitude influence of the quasi-biennial oscillation. *Quarterly Journal of the Royal Meteorological Society*, *140*(678), 1–21. https://doi.org/10.1002/qj.2132

Assani, A., Landry, R., & Laurencelle, M. (2012). Comparison of interannual variability modes and trends of seasonal precipitation and streamflow in southern Quebec (Canada). *River Research and Applications*, *28*(10), 1740–1752. https://doi.org/10.1002/rra.1544

Bailey, H., & Secor, D. H. (2016). Coastal evacuations by fish during extreme weather events. *Scientific Reports*, *6*(1), 1–9. https://doi.org/10.1038/srep30280

Baldwin, M., Gray, L., Dunkerton, T., Hamilton, K., Haynes, P., Randel, W., et al. (2001). The quasi-biennial oscillation. *Reviews of Geophysics*, *39*(2), 179–229. https://doi.org/10.1029/1999rg000073

Baldwin, M. P., & Dunkerton, T. J. (1999). Propagation of the Arctic oscillation from the stratosphere to the troposphere. *Journal of Geophysical Research*, *104*(D24), 30937–30946. https://doi.org/10.1029/1999jd900445

Boer, G., & Hamilton, K. (2008). QBO influence on extratropical predictive skill. *Climate Dynamics*, *31*(7), 987–1000. https://doi.org/10.1007/s00382-008-0379-5

Bonsal, B., & Shabbar, A. (2011). *Large-scale climate oscillations influencing Canada, 1900-2008*. Canadian Councils of Resource Ministers.

Bonsal, B., Zhang, X., Vincent, L., & Hogg, W. (2001). Characteristics of daily and extreme temperatures over Canada. *Journal of Climate*, *14*(9), 1959–1976. https://doi.org/10.1175/1520-0442(2001)014<1959:codaet>2.0.co;2

Bonsal, B. R., Shabbar, A., & Higuchi, K. (2001). Impacts of low frequency variability modes on Canadian winter temperature. *International Journal of Climatology: A Journal of the Royal Meteorological Society*, *21*(1), 95–108. https://doi.org/10.1002/joc.590

Chandran, A., Basha, G., & Ouarda, T. (2016). Influence of climate oscillations on temperature and precipitation over the United Arab Emirates. *International Journal of Climatology*, *36*(1), 225–235. https://doi.org/10.1002/joc.4339

Chattopadhyay, J., & Bhatla, R. (2002). Possible influence of QBO on teleconnections relating Indian summer monsoon rainfall and sea-surface temperature anomalies across the equatorial Pacific. *International Journal of Climatology: A Journal of the Royal Meteorological Society*, *22*(1), 121–127. https://doi.org/10.1002/joc.661

Cleveland, W. S. (1979). Robust locally weighted regression and smoothing scatterplots. *Journal of the American Statistical Association*, *74*(368), 829–836. https://doi.org/10.1080/01621459.1979.10481038

Cleveland, W. S. (1981). Lowess: A program for smoothing scatterplots by robust locally weighted regression. *The American Statistician*, *35*(1), 54. https://doi.org/10.2307/2683591

Cui, D., Liang, S., & Wang, D. (2021). Observed and projected changes in global climate zones based on Köppen climate classification. *Wiley Interdisciplinary Reviews: Climate Change*, *12*(3), e701. https://doi.org/10.1002/wcc.701

Currie, R. G. (1993). Luni-solar 18.6-and solar cycle 10–11-year signals in USA air temperature records. *International Journal of Climatology*, *13*(1), 31–50. https://doi.org/10.1002/joc.3370130103

Currie, R. G., & O'Brien, D. P. (1988). Periodic 18.6-year and cyclic 10 to 11 year signals in northeastern United States precipitation data. *Journal of Climatology*, *8*(3), 255–281. https://doi.org/10.1002/joc.3370080304

Currie, R. G., & Vines, R. G. (1996). Evidence for luni–solar and solar cycle signals in Australian rainfall data. *International Journal of Climatology*, *16*(11), 1243–1265. https://doi.org/10.1002/(sici)1097-0088(199611)16:11<1243::aid-joc85>3.0.co;2-e

D'Arrigo, R. D., Cook, E. R., Mann, M. E., & Jacoby, G. C. (2003). Tree-ring reconstructions of temperature and sea-level pressure variability associated with the warm-season Arctic Oscillation since AD 1650. *Geophysical Research Letters*, *30*(11), 1549. https://doi.org/10.1029/2003gl017250

Deng, Z., Qiu, X., Liu, J., Madras, N., Wang, X., & Zhu, H. (2016). Trend in frequency of extreme precipitation events over Ontario from ensembles of multiple GCMs. *Climate Dynamics*, *46*(9–10), 2909–2921. https://doi.org/10.1007/s00382-015-2740-9

Deser, C. (2000). On the teleconnectivity of the arctic oscillation. *Geophysical Research Letters*, *27*(6), 779–782. https://doi.org/10.1029/1999gl010945

Deser, C., Trenberth, K., & NCAR. (2016). The climate data guide: Pacific decadal oscillation (PDO): Definition and indices. [Dataset]. Retrieved from https://climatedataguide.ucar.edu/climate-data/pacific-decadal-oscillation-pdo-definition-and-indices

Dima, M., & Lohmann, G. (2007). A hemispheric mechanism for the atlantic multidecadal oscillation. *Journal of Climate*, *20*(11), 2706–2719. https://doi.org/10.1175/jcli4174.1

Dolney, T. J., & Sheridan, S. C. (2006). The relationship between extreme heat and ambulance response calls for the city of Toronto, Ontario, Canada. *Environmental Research*, *101*(1), 94–103. https://doi.org/10.1016/j.envres.2005.08.008

Dorothée. (2020). Red noise confidence levels. https://www.mathworks.com/matlabcentral/fileexchange/45539-rednoise_confidencelevels, MATLAB Central File Exchange. Retrieved February 11, 2020

Du, J., Wang, K., Wang, J., & Ma, Q. (2017). Contributions of surface solar radiation and precipitation to the spatiotemporal patterns of surface and air warming in China from 1960 to 2003. *Atmospheric Chemistry and Physics*, *17*(8), 4931–4944. https://doi.org/10.5194/acp-17-4931-2017

Dunkerton, T. J. (1997). The role of gravity waves in the quasi-biennial oscillation. *Journal of Geophysical Research*, *102*(D22), 26053–26076. https://doi.org/10.1029/96jd02999

Ebbesmeyer, C. C., Cayan, D. R., McLain, D. R., Nichols, F. H., Peterson, D. H., & Redmond, K. T. (1990). 1976 step in the Pacific climate: Forty environmental changes between. In J. L. Betancourt & V. L. Tharp (Eds.), *Proceedings of the 7th annual climate (PACLIM) workshop* (pp. 115–126). California Department of Water Resources.

Enfield, D. B., Mestas-Nuñez, A. M., & Trimble, P. J. (2001). The Atlantic Multidecadal Oscillation and its relation to rainfall and river flows in the continental US. *Geophysical Research Letters*, *28*(10), 2077–2080. https://doi.org/10.1029/2000gl012745

Environment and Climate Change Canada. (2020). Historical data. Retrieved from https://climate.weather.gc.ca/historical_data/search_historic_data_e.html

Feng, S., Hu, Q., & Oglesby, R. J. (2011). Influence of Atlantic sea surface temperatures on persistent drought in North America. *Climate Dynamics*, *37*(3–4), 569–586. https://doi.org/10.1007/s00382-010-0835-x

Fischer, P., & Tung, K. (2008). A reexamination of the QBO period modulation by the solar cycle. *Journal of Geophysical Research*, *113*(D7), D07114. https://doi.org/10.1029/2007jd008983

Frei, A., Kunkel, K. E., & Matonse, A. (2015). The seasonal nature of extreme hydrological events in the northeastern United States. *Journal of Hydrometeorology*, *16*(5), 2065–2085. https://doi.org/10.1175/jhm-d-14-0237.1

Fuentes-Franco, R., Giorgi, F., Coppola, E., & Kucharski, F. (2016). The role of ENSO and PDO in variability of winter precipitation over North America from twenty first century CMIP5 projections. *Climate Dynamics*, *46*(9–10), 3259–3277. https://doi.org/10.1007/s00382-015-2767-y

Gan, T. Y. (1995). Trends in air temperature and precipitation for Canada and north-eastern USA. *International Journal of Climatology*, *15*(10), 1115–1134. https://doi.org/10.1002/joc.3370151005

Gardner, A. S., Maclean, I. M., & Gaston, K. J. (2020). A new system to classify global climate zones based on plant physiology and using high temporal resolution climate data. *Journal of Biogeography*, *47*(10), 2091–2101. https://doi.org/10.1111/jbi.13927

Goly, A., & Teegavarapu, R. S. (2014). Individual and coupled influences of AMO and ENSO on regional precipitation characteristics and extremes. *Water Resources Research*, *50*(6), 4686–4709. https://doi.org/10.1002/2013wr014540

Goodrich, G. B., & Walker, J. M. (2011). The influence of the PDO on winter precipitation during high-and low-index ENSO conditions in the eastern United States. *Physical Geography*, *32*(4), 295–312. https://doi.org/10.2747/0272-3646.32.4.295

Gray, L. J., Anstey, J. A., Kawatani, Y., Lu, H., Osprey, S., & Schenzinger, V. (2018). Surface impacts of the quasi biennial oscillation. *Atmospheric Chemistry and Physics*, *18*(11), 8227–8247. https://doi.org/10.5194/acp-18-8227-2018

Grinsted, A., Moore, J. C., & Jevrejeva, S. (2004). Application of the cross wavelet transform and wavelet coherence to geophysical time series. *Nonlinear Processes in Geophysics*, *11*(5/6), 561–566. https://doi.org/10.5194/npg-11-561-2004

Groisman, P. Y., & Easterling, D. R. (1994). Variability and trends of total precipitation and snowfall over the United States and Canada. *Journal of Climate*, *7*(1), 184–205. https://doi.org/10.1175/1520-0442(1994)007<0184:vatotp>2.0.co;2

Hamilton, K. (2002). On the quasi-decadal modulation of the stratospheric QBO period. *Journal of Climate*, *15*(17), 2562–2565. https://doi.org/10.1175/1520-0442(2002)015<2562:otqdmo>2.0.co;2

Hare, S. R., & Mantua, N. J. (2000). Empirical evidence for North Pacific regime shifts in 1977 and 1989. *Progress in Oceanography*, *47*(2–4), 103–145. https://doi.org/10.1016/s0079-6611(00)00033-1

Hathaway, D. H. (2015). The solar cycle. *Living Reviews in Solar Physics*, *12*(1), 4. https://doi.org/10.1007/lrsp-2015-4

Holton, J. R., & Tan, H.-C. (1980). The influence of the equatorial quasi-biennial oscillation on the global circulation at 50 mb. *Journal of the Atmospheric Sciences*, *37*(10), 2200–2208. https://doi.org/10.1175/1520-0469(1980)037<2200:tioteq>2.0.co;2

Hu, Q., & Feng, S. (2012). AMO-and ENSO-driven summertime circulation and precipitation variations in North America. *Journal of Climate*, *25*(19), 6477–6495. https://doi.org/10.1175/jcli-d-11-00520.1

Huang, J., Hitchcock, P., Maycock, A. C., McKenna, C. M., & Tian, W. (2021). Northern hemisphere cold air outbreaks are more likely to be severe during weak polar vortex conditions. *Communications Earth & Environment*, *2*(1), 1–11. https://doi.org/10.1038/s43247-021-00215-6

Hurrell, J., & NCAR. (2020). The climate data guide: Hurrell North Atlantic oscillation (NAO) index (station-based). [dataset]. Retrieved from https://climatedataguide.ucar.edu/climate-data/hurrell-north-atlantic-oscillation-nao-index-station-based

Hurrell, J. W. (1995). Decadal trends in torth Atlantic oscillation: Regional temperatures and precipitation. *Science*, *269*(5224), 676–679. https://doi.org/10.1126/science.269.5224.676

Hurrell, J. W., Kushnir, Y., Ottersen, G., & Visbeck, M. (2003). An overview of the North Atlantic oscillation. *Geophysical Monograph-American Geophysical Union*, *134*, 1–36.

Hurrell, J. W., Kushnir, Y., & Visbeck, M. (2001). The north Atlantic oscillation. *Science*, *291*(5504), 603–605. https://doi.org/10.1126/science.1058761

Juanxiong, H., Zhihao, Y., & Xiuqun, Y. (2004). Temporal characteristics of Pacific decadal oscillation (PDO) and ENSO and their relationship analyzed with method of empirical mode decomposition (EMD). *Journal of Meteorological Research*, *19*, 83–92.

Knight, J. R., Folland, C. K., & Scaife, A. A. (2006). Climate impacts of the Atlantic multidecadal oscillation. *Geophysical Research Letters*, *33*(17), L17706. https://doi.org/10.1029/2006gl026242

Knudsen, M. F., Seidenkrantz, M.-S., Jacobsen, B. H., & Kuijpers, A. (2011). Tracking the Atlantic multidecadal oscillation through the last 8, 000 years. *Nature Communications*, *2*(1), 1–8. https://doi.org/10.1038/ncomms1186

Kopp, G. (2014). An assessment of the solar irradiance record for climate studies. *Journal of Space Weather and Space Climate*, *4*, A14. https://doi.org/10.1051/swsc/2014012

Kruskal, J. B. (1964). Nonmetric multidimensional scaling: A numerical method. *Psychometrika*, *29*(2), 115–129. https://doi.org/10.1007/bf02289694

Kuss, A. J. M., & Gurdak, J. J. (2014). Groundwater level response in US principal aquifers to ENSO, NAO, PDO, and AMO. *Journal of Hydrology*, *519*, 1939–1952. https://doi.org/10.1016/j.jhydrol.2014.09.069

Kwon, H.-H., Lall, U., Moon, Y.-I., Khalil, A. F., & Ahn, H. (2006). Episodic interannual climate oscillations and their influence on seasonal rainfall in the Everglades National Park. *Water Resources Research*, *42*(11). https://doi.org/10.1029/2006wr005017

Labat, D. (2008). Wavelet analysis of the annual discharge records of the world's largest rivers. *Advances in Water Resources*, *31*(1), 109–117. https://doi.org/10.1016/j.advwatres.2007.07.004

Lassen, K., & Friis-Christensen, E. (1995). Variability of the solar cycle length during the past five centuries and the apparent association with terrestrial climate. *Journal of Atmospheric and Terrestrial Physics*, *57*(8), 835–845. https://doi.org/10.1016/0021-9169(94)00088-6

Latif, M., & Barnett, T. P. (1994). Causes of decadal climate variability over the North Pacific and North America. *Science*, *266*(5185), 634–637. https://doi.org/10.1126/science.266.5185.634

Lau, K.-M., & Sheu, P. (1988). Annual cycle, quasi-biennial oscillation, and southern oscillation in global precipitation. *Journal of Geophysical Research*, *93*(D9), 10975–10988. https://doi.org/10.1029/jd093id09p10975

Laurenz, L., Lüdecke, H.-J., & Lüning, S. (2019). Influence of solar activity changes on European rainfall. *Journal of Atmospheric and Solar-Terrestrial Physics*, *185*, 29–42. https://doi.org/10.1016/j.jastp.2019.01.012

Le Goff, H., Flannigan, M. D., Bergeron, Y., & Girardin, M. P. (2007). Historical fire regime shifts related to climate teleconnections in the Waswanipi area, central Quebec, Canada. *International Journal of Wildland Fire*, *16*(5), 607–618. https://doi.org/10.1071/wf06151

Li, Z., Manson, A. H., Li, Y., & Meek, C. (2017). Circulation characteristics of persistent cold spells in central–eastern North America. *Journal of Meteorological Research*, *31*(1), 250–260. https://doi.org/10.1007/s13351-017-6146-y

Lim, Y.-K., & Schubert, S. D. (2011). The impact of ENSO and the Arctic Oscillation on winter temperature extremes in the southeast United States. *Geophysical Research Letters*, *38*(15). https://doi.org/10.1029/2011gl048283

Lindzen, R. S., & Holton, J. R. (1968). A theory of the quasi-biennial oscillation. *Journal of the Atmospheric Sciences*, *25*(6), 1095–1107. https://doi.org/10.1175/1520-0469(1968)025<1095:atotqb>2.0.co;2

Lockwood, M. (2012). Solar influence on global and regional climates. *Surveys in Geophysics*, *33*(3–4), 503–534. https://doi.org/10.1007/s10712-012-9181-3

Maliniemi, V., Asikainen, T., & Mursula, K. (2014). Spatial distribution of Northern Hemisphere winter temperatures during different phases of the solar cycle. *Journal of Geophysical Research: Atmospheres*, *119*(16), 9752–9764. https://doi.org/10.1002/2013jd021343

Mantua, N. J., & Hare, S. R. (2002). The Pacific decadal oscillation. *Journal of Oceanography*, *58*(1), 35–44. https://doi.org/10.1023/a:1015820616384

Marquardt Collow, A. B., Bosilovich, M. G., & Koster, R. D. (2016). Large-scale influences on summertime extreme precipitation in the northeastern United States. *Journal of Hydrometeorology*, *17*(12), 3045–3061. https://doi.org/10.1175/jhm-d-16-0091.1

McCabe, G. J., Palecki, M. A., & Betancourt, J. L. (2004). Pacific and Atlantic Ocean influences on multidecadal drought frequency in the United States. *Proceedings of the National Academy of Sciences*, *101*(12), 4136–4141. https://doi.org/10.1073/pnas.0306738101

McMichael, A. J. (2015). Extreme weather events and infectious disease outbreaks. *Virulence*, *6*(6), 543–547. https://doi.org/10.4161/21505594.2014.975022

Meehl, G. A., & Arblaster, J. M. (2009). A lagged warm event–like response to peaks in solar forcing in the Pacific region. *Journal of Climate*, *22*(13), 3647–3660. https://doi.org/10.1175/2009jcli2619.1

Meehl, G. A., Arblaster, J. M., Matthes, K., Sassi, F., & van Loon, H. (2009). Amplifying the Pacific climate system response to a small 11-year solar cycle forcing. *Science*, *325*(5944), 1114–1118. https://doi.org/10.1126/science.1172872

Mekis, É., & Vincent, L. A. (2011). An overview of the second generation adjusted daily precipitation dataset for trend analysis in Canada. *Atmosphere-Ocean*, *49*(2), 163–177. https://doi.org/10.1080/07055900.2011.583910

Mendoza, B., Lara, A., Maravilla, D., & Jáuregui, E. (2001). Temperature variability in central Mexico and its possible association to solar activity. *Journal of Atmospheric and Solar-Terrestrial Physics*, *63*(18), 1891–1900. https://doi.org/10.1016/s1364-6826(01)00075-x

Minobe, S. (1997). A 50–70 year climatic oscillation over the North Pacific and North America. *Geophysical Research Letters*, *24*(6), 683–686. https://doi.org/10.1029/97gl00504

Minobe, S. (1999). Resonance in bidecadal and pentadecadal climate oscillations over the North Pacific: Role in climatic regime shifts. *Geophysical Research Letters*, *26*(7), 855–858. https://doi.org/10.1029/1999gl900119

Moy, C. M., Seltzer, G. O., Rodbell, D. T., & Anderson, D. M. (2002). Variability of El niño/southern oscillation activity at millennial timescales during the holocene epoch. *Nature*, *420*(6912), 162–165. https://doi.org/10.1038/nature01194

Nalley, D., Adamowski, J., Biswas, A., Gharabaghi, B., & Hu, W. (2019). A multiscale and multivariate analysis of precipitation and streamflow variability in relation to ENSO, NAO and PDO. *Journal of Hydrology*, *574*, 288–307. https://doi.org/10.1016/j.jhydrol.2019.04.024

Nalley, D., Adamowski, J., & Khalil, B. (2012). Using discrete wavelet transforms to analyze trends in streamflow and precipitation in Quebec and Ontario (1954–2008). *Journal of Hydrology*, *475*, 204–228. https://doi.org/10.1016/j.jhydrol.2012.09.049

Nalley, D., Adamowski, J., Khalil, B., & Ozga-Zielinski, B. (2013). Trend detection in surface air temperature in Ontario and Quebec, Canada during 1967–2006 using the discrete wavelet transform. *Atmospheric Research*, *132*, 375–398. https://doi.org/10.1016/j.atmosres.2013.06.011

National Oceanic and Atmospheric Association. (2020). Climate data online. Retrieved from https://www.ncdc.noaa.gov/cdo-web/

NCAR. (2013). The climate data guide: Qbo: Quasi-biennial oscillation. [dataset]. Retrieved from https://climatedataguide.ucar.edu/climate-data/qbo-quasi-biennial-oscillation

NCAR. (2020). The climate data guide: Hurrell wintertime SLP-based northern annular mode (NAM) index. [Dataset]. Retrieved from https://climatedataguide.ucar.edu/climate-data/hurrell-wintertime-slp-based-northern-annular-mode-nam-index

Newman, M., Alexander, M. A., Ault, T. R., Cobb, K. M., Deser, C., Di Lorenzo, E., et al. (2016). The Pacific decadal oscillation, revisited. *Journal of Climate*, *29*(12), 4399–4427. https://doi.org/10.1175/jcli-d-15-0508.1

Newman, M., Compo, G. P., & Alexander, M. A. (2003). ENSO-forced variability of the Pacific decadal oscillation. *Journal of Climate*, *16*(23), 3853–3857. https://doi.org/10.1175/1520-0442(2003)016<3853:evotpd>2.0.co;2

Nigam, S., Barlow, M., & Berbery, E. H. (1999). Analysis links Pacific decadal variability to drought and streamflow in United States. EOS. *Transactions - American Geophysical Union*, *80*(51), 621–625. https://doi.org/10.1029/99eo00412

Ogurtsov, M. G., Raspopov, O. M., Helama, S., Oinonen, M., Lindholm, M., Jungner, H., & Meriläinen, J. (2008). Climatic variability along a north–south transect of Finland over the last 500 years: Signature of solar influence or internal climate oscillations? *Geografiska Annaler - Series A: Physical Geography*, *90*(2), 141–150. https://doi.org/10.1111/j.1468-0459.2008.00160.x

Olsen, J., Anderson, N. J., & Knudsen, M. F. (2012). Variability of The north Atlantic oscillation over the past 5, 200 years. *Nature Geoscience*, *5*(11), 808–812. https://doi.org/10.1038/ngeo1589

Overland, J., Hall, R., Hanna, E., Karpechko, A., Vihma, T., Wang, M., & Zhang, X. (2020). The polar vortex and extreme weather: The beast from the east in winter 2018. *Atmosphere*, *11*(6), 664. https://doi.org/10.3390/atmos11060664

Overland, J. E., & Wang, M. (2019). Impact of the winter polar vortex on greater North America. *International Journal of Climatology*, *39*(15), 5815–5821. https://doi.org/10.1002/joc.6174

Paterson, J. A., Ford, J. D., Ford, L. B., Lesnikowski, A., Berry, P., Henderson, J., & Heymann, J. (2012). Adaptation to climate change in the Ontario public health sector. *BMC Public Health*, *12*(1), 1–12. https://doi.org/10.1186/1471-2458-12-452

Patterson, R. T., & Swindles, G. T. (2015). Influence of ocean–atmospheric oscillations on lake ice phenology in eastern North America. *Climate Dynamics*, *45*(9–10), 2293–2308. https://doi.org/10.1007/s00382-014-2415-y

Philander, S. G. (1989). El Niño, La niña, and the southern oscillation. *International Geophysics Series*, *46*.

Philander, S. G. H. (1983). El Nino southern oscillation phenomena. *Nature*, *302*(5906), 295–301. https://doi.org/10.1038/302295a0

Quiroz, R. S. (1981). Period modulation of the stratospheric quasi-biennial oscillation. *Monthly Weather Review*, *109*(3), 665–674. https://doi.org/10.1175/1520-0493(1981)109<0665:pmotsq>2.0.co;2
Rao, J., Garfinkel, C. I., & Ren, R. (2019). Modulation of the northern winter stratospheric El niño–southern oscillation teleconnection by the PDO. *Journal of Climate*, *32*(18), 5761–5783. https://doi.org/10.1175/jcli-d-19-0087.1
Reid, S., Smit, B., Caldwell, W., & Belliveau, S. (2007). Vulnerability and adaptation to climate risks in Ontario agriculture. *Mitigation and Adaptation Strategies for Global Change*, *12*(4), 609–637. https://doi.org/10.1007/s11027-006-9051-8
Rind, D., Lean, J., Lerner, J., Lonergan, P., & Leboissitier, A. (2008). Exploring the stratospheric/tropospheric response to solar forcing. *Journal of Geophysical Research*, *113*(D24), D24103. https://doi.org/10.1029/2008jd010114
Rodionov, S., & Assel, R. A. (2003). Winter severity in the Great lakes region: A tale of two oscillations. *Climate Research*, *24*(1), 19–31. https://doi.org/10.3354/cr024019
Rogers, J., & McHugh, M. (2002). On the separability of the North Atlantic oscillation and Arctic oscillation. *Climate Dynamics*, *19*(7), 599–608. https://doi.org/10.1007/s00382-002-0247-7
Ropelewski, C. F., & Halpert, M. S. (1986). North American precipitation and temperature patterns associated with the El Niño/Southern Oscillation (ENSO). *Monthly Weather Review*, *114*(12), 2352–2362. https://doi.org/10.1175/1520-0493(1986)114<2352:napatp>2.0.co;2
Ruiz-Barradas, A., Nigam, S., & Kavvada, A. (2013). The Atlantic multidecadal oscillation in twentieth century climate simulations: Uneven progress from CMIP3 to CMIP5. *Climate Dynamics*, *41*(11–12), 3301–3315. https://doi.org/10.1007/s00382-013-1810-0
Schlesinger, M. E., & Ramankutty, N. (1994). An oscillation in the global climate system of period 65–70 years. *Nature*, *367*(6465), 723–726. https://doi.org/10.1038/367723a0
Schulz, M., & Mudelsee, M. (2002). Redfit: Estimating red-noise spectra directly from unevenly spaced paleoclimatic time series. *Computers & Geosciences*, *28*(3), 421–426. https://doi.org/10.1016/s0098-3004(01)00044-9
Seager, R., Kushnir, Y., Nakamura, J., Ting, M., & Naik, N. (2010). Northern hemisphere winter snow anomalies: ENSO, NAO and the winter of 2009/10. *Geophysical Research Letters*, *37*(14). https://doi.org/10.1029/2010gl043830
Sfîcă, L., Iordache, I., & Voiculescu, M. (2018). Solar signal on regional scale: A study of possible solar impact upon Romania's climate. *Journal of Atmospheric and Solar-Terrestrial Physics*, *177*, 257–265. https://doi.org/10.1016/j.jastp.2017.09.015
Sharma, S., & Magnuson, J. J. (2014). Oscillatory dynamics do not mask linear trends in the timing of ice breakup for Northern Hemisphere lakes from 1855 to 2004. *Climatic Change*, *124*(4), 835–847. https://doi.org/10.1007/s10584-014-1125-0
Shephard, M. W., Mekis, E., Morris, R. J., Feng, Y., Zhang, X., Kilcup, K., & Fleetwood, R. (2014). Trends in Canadian short-duration extreme rainfall: Including an intensity–duration–frequency perspective. *Atmosphere-Ocean*, *52*(5), 398–417. https://doi.org/10.1080/07055900.2014.969677
SILSO. (2021). Total sunspot number. [Dataset]. Royal Observatory of Belgium. Retrieved from http://www.sidc.be/silso
Smith, E. T., & Sheridan, S. C. (2019). The influence of extreme cold events on mortality in the United States. *Science of the Total Environment*, *647*, 342–351. https://doi.org/10.1016/j.scitotenv.2018.07.466
Soulis, E., Sarhadi, A., Tinel, M., & Suthar, M. (2016). Extreme precipitation time trends in Ontario, 1960–2010. *Hydrological Processes*, *30*(22), 4090–4100. https://doi.org/10.1002/hyp.10969
Stockwell, J. D., Doubek, J. P., Adrian, R., Anneville, O., Carey, C. C., Carvalho, L., et al. (2020). Storm impacts on phytoplankton community dynamics in lakes. *Global Change Biology*, *26*(5), 2756–2784. https://doi.org/10.1111/gcb.15033
Tan, X., Gan, T. Y., & Shao, D. (2016). Wavelet analysis of precipitation extremes over Canadian ecoregions and teleconnections to large-scale climate anomalies. *Journal of Geophysical Research: Atmospheres*, *121*(24), 14–469. https://doi.org/10.1002/2016jd025533
Thiombiano, A. N., ElAdlouni, S., St-Hilaire, A., Ouarda, T. B., & El-Jabi, N. (2017). Nonstationary frequency analysis of extreme daily precipitation amounts in Southeastern Canada using a peaks-over-threshold approach. *Theoretical and Applied Climatology*, *129*(1–2), 413–426. https://doi.org/10.1007/s00704-016-1789-7
Thompson, D. W., & Wallace, J. M. (1998). The Arctic Oscillation signature in the wintertime geopotential height and temperature fields. *Geophysical Research Letters*, *25*(9), 1297–1300. https://doi.org/10.1029/98gl00950
Thomson, D. J. (1982). Spectrum estimation and harmonic analysis. *Proceedings of the IEEE*, *70*(9), 1055–1096. https://doi.org/10.1109/proc.1982.12433
Toniazzo, T., & Scaife, A. A. (2006). The influence of ENSO on winter North Atlantic climate. *Geophysical Research Letters*, *33*(24), L24704. https://doi.org/10.1029/2006gl027881
Torrence, C., & Compo, G. P. (1998). A practical guide to wavelet analysis. *Bulletin of the American Meteorological Society*, *79*(1), 61–78. https://doi.org/10.1175/1520-0477(1998)079<0061:apgtwa>2.0.co;2
Trenberth, K., & NCAR. (2020). The climate data guide: Nino sst indices (nino 1+2, 3, 3.4, 4; oni and tni). [Dataset]. Retrieved from https://climatedataguide.ucar.edu/climate-data/nino-sst-indices-nino-12-3-34-4-oni-and-tni
Trenberth, K., Zhang, R., & NCAR. (2021). The climate data guide: Atlantic multi-decadal oscillation. [dataset]. Retrieved from https://climatedataguide.ucar.edu/climate-data/atlantic-multi-decadal-oscillation-amo
Trenberth, K. E. (1990). Recent observed interdecadal climate changes in the Northern Hemisphere. *Bulletin of the American Meteorological Society*, *71*(7), 988–993. https://doi.org/10.1175/1520-0477(1990)071<0988:roicci>2.0.co;2
Valdés-Pineda, R., Cañón, J., & Valdés, J. B. (2018). Multi-decadal 40-to 60-year cycles of precipitation variability in Chile (South America) and their relationship to the AMO and PDO signals. *Journal of Hydrology*, *556*, 1153–1170. https://doi.org/10.1016/j.jhydrol.2017.01.031
Van de Pol, M., Jenouvrier, S., Cornelissen, J. H., & Visser, M. E. (2017). *Behavioural, ecological and evolutionary responses to extreme climatic events: Challenges and directions*. The Royal Society.
van Loon, H., Meehl, G. A., & Arblaster, J. M. (2004). A decadal solar effect in the tropics in July–August. *Journal of Atmospheric and Solar-Terrestrial Physics*, *66*(18), 1767–1778. https://doi.org/10.1016/j.jastp.2004.06.003
van Loon, H., & Shea, D. J. (1999). A probable signal of the 11-year solar cycle in the troposphere of the Northern Hemisphere. *Geophysical Research Letters*, *26*(18), 2893–2896. https://doi.org/10.1029/1999gl900596
Vincent, L., Zhang, X., Mekis, É., Wan, H., & Bush, E. (2018). Changes in Canada's climate: Trends in indices based on daily temperature and precipitation data. *Atmosphere-Ocean*, *56*(5), 332–349. https://doi.org/10.1080/07055900.2018.1514579
Vines, R. (1977). Possible relationships between rainfall, crop yields and the Sunspot cycle. *Journal of the Australian Institute of Agricultural Science*, *43*(1–2), 3–13.
Vines, R. (1980). Analyses of South African rainfall. *South African Journal of Science*, *76*(9), 404–409.
Vines, R. (1984). Rainfall patterns in the eastern United States. *Climatic Change*, *6*(1), 79–98. https://doi.org/10.1007/bf00141669
Walsh, C. R., & Patterson, R. T. (2022). Precipitation and temperature trends and cycles derived from historical 1890–2019 weather data for the city of ottawa, Ontario, Canada. *Environments*, *9*(3), 35. https://doi.org/10.3390/environments9030035

Walter, K., & Graf, H.-F. (2005). The North Atlantic variability structure, storm tracks, and precipitation depending on the polar vortex strength. *Atmospheric Chemistry and Physics*, *5*(1), 239–248. https://doi.org/10.5194/acp-5-239-2005

Wang, D., Wang, C., Yang, X., & Lu, J. (2005). Winter northern hemisphere surface air temperature variability associated with the arctic oscillation and north atlantic oscillation. *Geophysical Research Letters*, *32*(16), L16706. https://doi.org/10.1029/2005gl022952

Wang, J., Kessler, J., Bai, X., Clites, A., Lofgren, B., Assuncao, A., et al. (2018). Decadal variability of Great Lakes ice cover in response to AMO and PDO, 1963–2017. *Journal of Climate*, *31*(18), 7249–7268. https://doi.org/10.1175/jcli-d-17-0283.1

Wang, X., Thompson, D. K., Marshall, G. A., Tymstra, C., Carr, R., & Flannigan, M. D. (2015). Increasing frequency of extreme fire weather in Canada with climate change. *Climatic Change*, *130*(4), 573–586. https://doi.org/10.1007/s10584-015-1375-5

Ward, J. H., Jr. (1963). Hierarchical grouping to optimize an objective function. *Journal of the American Statistical Association*, *58*(301), 236–244. https://doi.org/10.1080/01621459.1963.10500845

World Economic Forum. (2019). *The global risks report* (14th ed.). World Economic Forum.

Yagouti, A., Boulet, G., Vincent, L., Vescovi, L., & Mekis, E. (2008). Observed changes in daily temperature and precipitation indices for southern Québec, 1960–2005. *Atmosphere-Ocean*, *46*(2), 243–256. https://doi.org/10.3137/ao.460204

Yang, R., Cao, J., Huang, W., & Nian, A. (2010). Cross wavelet analysis of the relationship between total solar irradiance and sunspot number. *Chinese Science Bulletin*, *55*(20), 2126–2130. https://doi.org/10.1007/s11434-010-3269-2

Yang, Y., Gan, T. Y., & Tan, X. (2019). Spatiotemporal changes in precipitation extremes over Canada and their teleconnections to large-scale climate patterns. *Journal of Hydrometeorology*, *20*(2), 275–296. https://doi.org/10.1175/jhm-d-18-0004.1

Zhang, G., Zeng, G., Li, C., & Yang, X. (2020). Impact of PDO and AMO on interdecadal variability in extreme high temperatures in North China over the most recent 40-year period. *Climate Dynamics*, *54*(5), 3003–3020. https://doi.org/10.1007/s00382-020-05155-z

Zhang, W., Mei, X., Geng, X., Turner, A. G., & Jin, F.-F. (2019). A nonstationary ENSO–NAO relationship due to AMO modulation. *Journal of Climate*, *32*(1), 33–43. https://doi.org/10.1175/jcli-d-18-0365.1

Zhang, X., Hogg, W., & Mekis, É. (2001). Spatial and temporal characteristics of heavy precipitation events over Canada. *Journal of Climate*, *14*(9), 1923–1936. https://doi.org/10.1175/1520-0442(2001)014<1923:satcoh>2.0.co;2

Zhang, X., Vincent, L. A., Hogg, W., & Niitsoo, A. (2000). Temperature and precipitation trends in Canada during the 20th century. *Atmosphere-Ocean*, *38*(3), 395–429. https://doi.org/10.1080/07055900.2000.9649654

Zhang, X., Wang, J., Zwiers, F. W., & Groisman, P. Y. (2010). The influence of large-scale climate variability on winter maximum daily precipitation over North America. *Journal of Climate*, *23*(11), 2902–2915. https://doi.org/10.1175/2010jcli3249.1

Zhang, X., Yan, X., & Chen, Z. (2017). Geographic distribution of global climate zones under future scenarios. *International Journal of Climatology*, *37*(12), 4327–4334. https://doi.org/10.1002/joc.5089

Zhao, H., Higuchi, K., Waller, J., Auld, H., & Mote, T. (2013). The impacts of the PNA and NAO on annual maximum snowpack over southern Canada during 1979–2009. *International Journal of Climatology*, *33*(2), 388–395. https://doi.org/10.1002/joc.3431

Znachor, P., Zapomělová, E., Řeháková, K., Nedoma, J., & Šimek, K. (2008). The effect of extreme rainfall on summer succession and vertical distribution of phytoplankton in a lacustrine part of a eutrophic reservoir. *Aquatic Sciences*, *70*(1), 77–86. https://doi.org/10.1007/s00027-007-7033-x